- 11.5 A cavity for a 6328-Å He-Ne laser is 50 cm long with reflection coefficient $r_1 = 1.0$ for one mirror and $r_2 = 0.98$ for the other. Losses other than output coupling are very small and may be ignored. The output power of the laser is measured to be about 10-mW on a single mode.
 - (a) What is the cavity photon number and what is the output rate of photons?
 - (b) It has been written that "if the light from a thousand suns were to shine in the sky, that would be the glory of the Mighty One." Assume that the sun is an ideal blackbody radiator at T=6000 K. Estimate the flux of photons in a frequency band of width $\delta \nu \approx 10$ MHz centered at 6328 Å that can be obtained from 1000 suns. How does this compare with the photon flux that can be obtained from He-Ne or other lasers?
- 11.6 Should the Lamb dip occur with any inhomogeneously broadened gain medium, or only the specific case of Doppler broadening?
- 11.7 Do you think that most lasers have a cavity bandwidth much larger or smaller than the linewidth of the gain profile? Is any implicit assumption about this made in our discussion related to Figure 11.13?
- 11.8 Derive Eq. (11.12.5) for the resonance frequencies of a Fabry-Perot etalon for an arbitrary angle of incidence.

12 MULTIMODE AND TRANSIENT OSCILLATION

12.1 INTRODUCTION

Thus far we have restricted our study of the laser to the case of continuous-wave, single-mode operation. In this chapter we will consider time-dependent, transient effects, including relaxation oscillations and Q switching. We will also extend our single-mode theory somewhat to the case in which several or many cavity modes can oscillate simultaneously. This allows us in particular to understand the important technique called mode locking, a way to obtain ultrashort pulses of light.

12.2 RATE EQUATIONS FOR INTENSITIES AND POPULATIONS

In the preceding two chapters we have found it convenient and instructive to describe the strength of the cavity field either in terms of intensity I_{ν} or photon number q_{ν} . In the present chapter it will be convenient to use the intensity description. We will therefore begin with a brief review of the appropriate equations coupling the intensity and the laser level population densities N_2 and N_1 .

In general the cavity intensity will vary both in time and space. We will continue in this chapter to make the plane-wave approximation in which the intensity is assumed to be uniform in any plane perpendicular to the cavity axis. Furthermore we showed in Section 11.5 that, for the most common situation in which the mirror reflectivities are large (say, >50%), the cavity intensity is approximately uniform along the cavity axis if we ignore the rapidly varying $\sin^2 kz$ interference term. So it is useful again to make the uniform-field approximation, but now to include the time dependence of the cavity intensity. First we recall equation (10.5.8):

$$\frac{dI_{\nu}}{dt} = \frac{cl}{L} \left(g(\nu) I_{\nu} - \frac{1}{2l} (1 - r_1 r_2) I_{\nu} \right)$$

$$= \frac{cl}{L} \left[g(\nu) - g_t \right] I_{\nu} \tag{12.2.1}$$

For simplicity we will assume that the gain cell fills the entire space between the mirrors. Then l=L and

$$\frac{dI_{\nu}}{dt} = c \left[g(\nu) - g_t \right] I_{\nu} \tag{12.2.2}$$

Recall that $I_{\nu} = I_{\nu}^{(+)} + I_{\nu}^{(-)}$ is the sum of the two traveling-wave intensities; in the case of high mirror reflectivities, the two are approximately equal.

In terms of the cavity intensity we can write the population rate equations [cf. (10.5.14) with $\Gamma_1 = \Gamma_2 = 0$ and $A \rightarrow \Gamma_{21}$

$$\frac{dN_2}{dt} = -\frac{g(\nu)I_{\nu}}{h\nu} - \Gamma_{21}N_2 + K_2$$
 (12.2.3a)

$$\frac{dN_1}{dt} = \frac{g(\nu)I_{\nu}}{h\nu} + \Gamma_{21}N_2 + K_1 \tag{12.2.3b}$$

where the rates Γ_{21} , K_2 , and K_1 are, again, level decay and pumping rates. Since N_2 and N_1 are populations per unit volume, the pumping rates have units of (volume)⁻¹ (time)⁻¹. Equations (12.2.2) and (12.2.3) are coupled rate equations for I_{ν} , N_2 , and N_1 . The coupling is through the gain coefficient

$$g(\nu) = \frac{\lambda^2 A}{8\pi} (N_2 - N_1) S(\nu)$$

= $\sigma(\nu) (N_2 - N_1)$ (12.2.4)

where we assume for simplicity that $g_2/g_1 = 1$.

The population rate equations (12.2.3) are easily modified to suit a particular laser medium. We have already described such modifications in the case of the stylized three- and four-level models. Further modifications are described in Chapter 13, where we consider specific population inversion mechanisms. Since we will be describing in this chapter some rather general phenomena that transcend specific inversion schemes, it will be adequate to use the simple rate equations (12.2.3) for the laser level population densities.

For many purposes the rate equations (12.2.2) and (12.2.3) may be simplified somewhat. One simplifying assumption is that $N_1 \ll N_2$, i.e., that the lower laser level population is negligible compared with the upper laser level population. This would be the case in a four-level laser, where the lower level decays very rapidly compared with the stimulated emission (absorption) rate. Then $g(\nu) = \sigma(\nu) N_2$, and (12.2.2) and (12.2.3a) become

$$\frac{dI_{\nu}}{dt} = c\sigma(\nu) N_2 I_{\nu} - cg_t I_{\nu}$$
 (12.2.5a)

$$\frac{dN_2}{dt} = -\frac{\sigma(\nu)}{h\nu} N_2 I_{\nu} - \Gamma_{21} N_2 + K_2$$
 (12.2.5b)

RELAXATION OSCILLATIONS

The coupled equations (12.2.5) for I_{ν} and N_2 are simple in appearance, but they have no known general solution. However, it is easy to find the steady-state solutions which we denote \overline{I}_{ν} and \overline{N}_{2} . These are obtained simply by replacing the left sides of (12.2.5) by zero and solving the resulting algebraic equations, with the result

$$\bar{I}_{\nu} = h\nu \left(\frac{K_2}{g_t} - \frac{\Gamma_{21}}{\sigma(\nu)}\right) \tag{12.3.1a}$$

$$\overline{N}_2 = \frac{g_t}{\sigma(\nu)} \tag{12.3.1b}$$

These solutions may also be written in a different form to show explicitly how N_2 saturates with increasing \bar{I}_{ν} (Problem 12.1).

It is possible to solve these equations approximately if the laser is operating very near to steady state. In this case we write

$$I_{\nu} = \bar{I}_{\nu} + \epsilon \tag{12.3.2a}$$

$$N_2 = \overline{N}_2 + \eta \tag{12.3.2b}$$

and assume

$$|\epsilon| \ll \bar{I}_{\nu} \tag{12.3.3a}$$

$$|\eta| \ll \overline{N}_2 \tag{12.3.3b}$$

This approximation allows the equations (12.2.5) to be linearized and solved, as follows.

Using (12.3.2) in (12.2.5a), we have

$$\frac{d}{dt}(\bar{I}_{\nu}+\epsilon)=c\sigma(\bar{N}_{2}+\eta)(\bar{I}_{\nu}+\epsilon)-cg_{t}(\bar{I}_{\nu}+\epsilon) \qquad (12.3.4)$$

which is the same (since $d\bar{I}_{\nu}/dt = 0$) as

$$\frac{d\epsilon}{dt} = c\sigma(\overline{N}_2 + \eta)(\overline{I}_{\nu} + \epsilon) - cg_t(\overline{I}_{\nu} + \epsilon)$$

$$= c\sigma(\overline{N}_2\overline{I}_{\nu} + \overline{N}_2\epsilon + \eta\overline{I}_{\nu} + \eta\epsilon) - cg_t(\overline{I}_{\nu} + \epsilon) \qquad (12.3.5)$$

Now \overline{I}_{ν} and \overline{N}_{2} are such as to make the right sides of (12.2.5) vanish. In particular,

$$c\sigma \overline{N}_2 \overline{I}_{\nu} - cg_t \overline{I}_{\nu} = 0 \tag{12.3.6}$$

Using this relation in (12.3.5), we obtain the much simpler equation

$$\frac{d\epsilon}{dt} = c\sigma\eta \,\bar{I}_{\nu} + c\sigma\eta\epsilon \tag{12.3.7}$$

This is still nonlinear (because of the term $\eta\epsilon$), but now the nonlinearity is very small because it involves the product of the small quantities η and ϵ . Near enough to steady state [recall (12.3.3)], such second-order-small terms can be dropped altogether without significant error. Thus we obtain the following linear equation for the time dependence of the departure of the cavity intensity from its steady-state value:

$$\frac{d\epsilon}{dt} = (c\sigma \bar{I}_{\nu})\eta \tag{12.3.8}$$

where the factor in parentheses is constant in time.

The same procedure can be applied to (12.2.5b). Again the product $\eta\epsilon$ is very small and can be dropped, and again the definitions of \tilde{I}_{ν} and N_2 can be used to cancel some terms. The result is

$$\frac{d\eta}{dt} = -\frac{g_t}{h\nu} \epsilon - \frac{\sigma K_2}{g_t} \eta \tag{12.3.9}$$

Equations (12.3.8) and (12.3.9) are still coupled to each other, but they are now linear and easily solved. We use (12.3.8) to replace η in (12.3.9) by $(c\sigma I_{\nu})^{-1}$ $d\epsilon/dt$ to get

$$\frac{d^2\epsilon}{dt^2} + \gamma \frac{d\epsilon}{dt} + \omega_0^2 \epsilon = 0 \tag{12.3.10}$$

where we define

$$\gamma = \sigma K_2/g_t \tag{12.3.11}$$

and

$$\omega_0^2 = \frac{c\sigma g_t}{h\nu} \bar{I}_{\nu} \tag{12.3.12}$$

The solution to (12.3.10) is easily found to be

$$\epsilon(t) = A e^{-\gamma t/2} \cos(\omega t + \phi) \tag{12.3.13}$$

where A and ϕ are the initial amplitude and phase of $\epsilon(t)$, and the frequency of oscillation is given by

$$\omega = \sqrt{\omega_0^2 - \frac{\gamma^2}{4}} \tag{12.3.14}$$

For definiteness we assume $\omega_0 > \gamma/2$, making ω real. Thus, near to the steady

state, the cavity intensity oscillates about the steady-state value \bar{I}_{ν} , and gradually approaches \bar{I}_{ν} at the (exponential) rate $\gamma/2$:

$$I_{\nu} = \bar{I}_{\nu} + A e^{-\gamma t/2} \cos(\omega t + \phi)$$
 (12.3.15)

This is called a *relaxation oscillation*. Similar behavior is observed in a wide variety of nonlinear systems.

Although the relaxation-oscillation solution (12.3.13) is valid only if $|\epsilon| \ll \bar{I}_{\nu}$ [recall (12.3.3)], the nature of the solution is of general importance. The critical feature of the solution is that γ is positive. This guarantees that the steady-state solution \bar{I}_{ν} is a *stable* solution. That is, if some outside agent slightly disturbs the laser while it is running in steady state, the effect of the disturbance decays to zero, thus returning the laser to steady state again. If γ were negative, a small disturbance would grow, and the steady state would therefore be unstable, and thus of very little practical significance.

We may write the period T_r and lifetime τ_r of the relaxation oscillations as (Problem 12.1)

$$T_r = \frac{2\pi}{\omega_0} = \frac{2\pi}{\sqrt{(c/\tau_{21})(g_0 - g_t)}}$$
 (12.3.16)

and

$$\tau_r = \frac{1}{\gamma} = \frac{g_t}{g_0} \, \tau_{21} \tag{12.3.17}$$

where g_0 is the small-signal gain and $\tau_{21} = \Gamma_{21}^{-1}$ is the lifetime of the upper laser level. From (12.3.17) or (12.3.11) we see that the duration of the relaxation oscillations decreases with increasing pumping rate K_2 of the gain medium. Likewise the period T_r of the relaxation oscillations should decrease with increased g_0 . These predicted trends are consistent with many experimental observations.

It is possible to observe relaxation oscillations in the output intensity of a laser after it is turned on and approaches a steady-state operation. Perturbations in the pumping power can also cause relaxation oscillations to appear spontaneously. In some cases, especially in solid-state lasers, the relaxation time τ_r may be relatively large, making relaxation oscillations readily apparent on an oscilloscope trace of the laser output intensity.

As an example, consider a ruby laser with mirror reflectivities $r_1 \approx 1.0$, $r_2 \approx 0.94$, and a ruby rod of length l = 5.0 cm. For such a laser $g_t \approx (1/2l) (1 - r_2) = 0.006$ cm⁻¹, so that $cg_t \approx 1.8 \times 10^8$ sec⁻¹. For ruby the upper level lifetime $\tau_{21} \approx 2 \times 10^{-3}$ sec. Assuming a pumping level such that $g_0/g_t = 2.0$, we compute from (12.3.16) and (12.3.17) the period and lifetime of relaxation oscillations:

$$T_r \approx 21 \,\mu\,\text{sec} \tag{12.3.18}$$

$$\tau_r \approx 2 \text{ msec}$$
 (12.3.19)

Relaxation-oscillation periods are often in the microsecond range, as in this example. The damping time τ_r is particularly large in ruby because of its unusually long upper-level lifetime τ_{21} . Relaxation oscillations are therefore particularly pronounced in ruby. The output of a continuously pumped ruby laser typically consists of a series of irregular spikes, and this spiking behavior is usually attributed to relaxation oscillations being continuously excited by various mechanical and thermal perturbations.

12.4 Q SWITCHING

Q switching is a way of obtaining short, powerful pulses of laser radiation. Q refers to the quality factor of the laser resonator, as discussed in Section 11.9; recall that a high-Q cavity is one with low loss, whereas a "lossy" cavity will have a low Q. The term Q switching therefore refers to an abrupt change in the cavity loss. Specifically, it is a sudden switching of the cavity Q from a low value to a high value, i.e., a sudden lowering of the cavity loss. In this section we will describe how Q switching works, and in the following section how it is achieved in actual lasers.

Suppose we pump a laser medium inside a very lossy cavity. Because the loss is so large, laser action is precluded even if the upper level population N_2 is pumped to a very high value. No field builds up by stimulated emission in the gain cell. Obviously this means that the gain cannot be saturated, and if pumping is very strong it can grow to a large, small-signal value. Suddenly we lower the loss to a value permitting laser oscillation. We now have a small-signal gain much larger than the threshold gain for oscillation.

What happens in this situation, of course, is that there is a rapid growth of intensity inside the cavity. The intensity builds up quickly to a large value, resulting in a large stimulated emission rate and therefore a rapid extraction of energy from the gain cell. The result of the Q switching is therefore a short, intense pulse of laser radiation, sometimes called a *giant pulse*. Pulses as short as 10^{-7} – 10^{-8} sec are routinely obtained by Q switching.

This qualitative explanation of Q switching may be substantiated by solving the rate equations (12.2.5). For this purpose it is convenient to define the dimensionless quantities

$$x = \frac{I_{\nu}}{ch\nu N_{t}} \tag{12.4.1}$$

$$y = \frac{N_2}{N_t}$$
 (12.4.2)

where N_t is the threshold population inversion density. The threshold gain is $g_t = \sigma(\nu) N_t$. Clearly y is the ratio of the population inversion to the threshold inversion, or, equivalently, the ratio of gain g to threshold gain g_t ; and x is easily shown

to be the ratio of the cavity photon density to the threshold population inversion density (Problem 12.2).

In terms of x, y, and the dimensionless time variable

$$\tau = cg_t t \tag{12.4.3}$$

the equation (12.2.5a) for the cavity intensity takes the form (Problem 12.2)

$$\frac{dx}{d\tau} = (y - 1)x\tag{12.4.4a}$$

We will assume that the duration of the "giant pulse" is short enough that pumping and spontaneous decay of N_2 during this interval is negligible, and only stimulated decay due to the intense pulse occurs. This assumption allows us to ignore the second and third terms on the right side of the rate equation (12.2.5b), and to write the simpler equation (Problem 12.2)

$$\frac{dy}{d\tau} = -xy \tag{12.4.4b}$$

The validity of this assumption can always be checked after a solution of equations (12.4.4) has been obtained.

The result of a numerical integration of equations (12.4.4) is shown in Figure 12.1. The pumping level prior to Q switching is assumed to be such that y(0) = 2. We observe that the normalized intensity x grows until the population inversion drops below threshold, at which point the intensity begins to decrease.

As a specific example, consider the case of a 6943-Å ruby laser, in which $\sigma \approx 2.7 \times 10^{-20}$ cm². Suppose one of the mirrors is highly reflecting $(r_1 \approx 1.0)$, the other has a reflectivity $r \approx 0.90$, and the ruby rod has a length l = 5 cm. Then

$$g_t \approx \frac{1}{2l} (1 - r) = 0.01 \text{ cm}^{-1}$$
 (12.4.5)

and $cg_r \approx 3 \times 10^8 \text{ sec}^{-1}$. From (12.4.3), therefore,

$$\tau = 3 \times 10^8 t$$
 (t measured in seconds) (12.4.6)

The Q-switched pulse of Figure 12.1 has a width of about $\tau = 4$, corresponding to an actual pulse duration of

$$t_p = (3 \times 10^8)^{-1} (4) = 13 \text{ nsec}$$
 (12.4.7)

The variable x in Figure 12.1 has a peak value of about 0.3, corresponding to a peak intensity of [Eq. (12.4.1)]

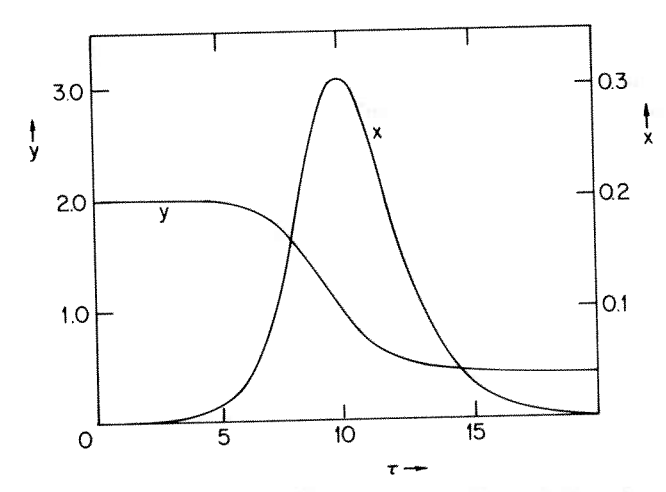


Figure 12.1 Solution of Eqs. (12.4.4) for y(0) = 2 and $x(0) \approx 0$.

$$I_{\text{peak}} = (ch\nu) N_t (0.3) = \left(\frac{c^2 h}{\lambda}\right) \left(\frac{g_t}{\sigma}\right) (0.3)$$

$$\approx 10^9 \text{ W/cm}^2 \qquad (12.4.8)$$

as the reader may easily verify. This is a very large amount of power—much larger than would be obtainable if the same laser were operated as a continuous-wave device (Problem 12.3). For a beam cross-sectional area of 0.1 cm^2 the total energy in the Q-switched pulse is

energy
$$\approx (I_{\text{peak}}) (t_p) (0.1 \text{ cm}^2)$$

 $\approx 1 \text{ J}$ (12.4.9)

• Equations (12.4.4) imply that, if x(0) = 0, then x and y remain fixed at their initial values. Physically, this is incorrect, and occurs only because in writing (12.4.4) we left out the effect of spontaneous emission. Spontaneous emission has the effect of giving x a small but nonzero initial value, allowing it to grow from this initial value. In other words, spontaneous emission provides the first few "seed" photons needed to initiate the growth of laser intensity by stimulated emission.

In obtaining the numerical results shown in Figure 12.1 a fourth-order Runge-Kutta integration algorithm was used, with a step size $\Delta \tau = 0.01$. An initial value of 10^{-4} was assumed for x(0). The numerical results for the pulse shape, duration, and peak value are insensitive to the (small) initial value assumed for x. This is because x grows to values large compared with its initial value. Then the number of cavity photons becomes so large that spontaneous emission is negligible compared with stimulated emission.

The value of τ at which the pulse intensity reaches its peak, however, does depend upon the choice of x(0). If this aspect of the problem is of concern, therefore, one should include

properly the effect of spontaneous emission in the rate equations (12.4.4) as well as various details of the Q switching.

The reader may wish to experiment with Eqs. (12.4.4), or various other differential equations that appear in this book and in the laser research literature. We include in Appendix 12.A both BASIC and FORTRAN listings of the Runge-Kutta algorithm used to obtain the results in Figure 12.1. •

12.5 METHODS OF Q SWITCHING

There are various ways to Q-switch a laser. The most popular ones switch the cavity Q factor within a time interval that is short compared with the photon lifetime $(cg_t)^{-1}$, allowing the gain to build up to a large value before the onset of laser oscillation. We will discuss three common methods of Q switching.

Rotating Mirrors

One way to Q-switch is to have one of the cavity mirrors rotating about an axis perpendicular to the cavity axis (Figure 12.2). The loss is then very large except during the brief period when the mirrors are nearly parallel. A typical angular velocity of the rotating mirror is about 10,000 revolutions per minute (rpm).

A similar mechanical method of Q switching involves a rotating chopper wheel. In this method, however, the Q switching is effected relatively slowly, even for a wheel velocity of 10,000 rpm. This is because lasing can begin before the shutter fully exposes the gain cell to the cavity mirrors.

Electro-optical Switches

Electro-optical shutters can be used to control the cavity Q by means of an applied voltage. To understand the operation of these switches, we must first describe the electro-optical effect. In Section 2.9 we identified birefringence as a difference in refractive indices for light of different linear polarizations. The electro-optical effect refers to birefringence that occurs in certain media when a voltage is applied. One example is the Kerr effect, in which the degree of birefringence is proportional to the square of the applied voltage. Another is the Pockels effect, in which the birefringence is linearly proportional to the voltage. Kerr cells typically require voltages in the 10-20 kilovolt range and Pockels cells somewhat less.

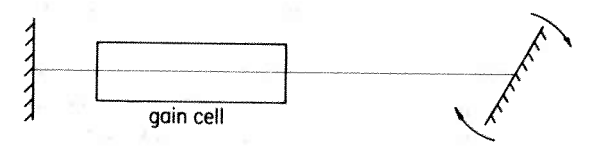


Figure 12.2 A laser cavity with a rotating mirror for Q switching.

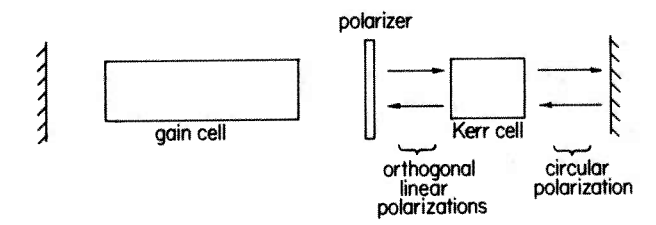


Figure 12.3 Q switching with a Kerr cell. With the Kerr cell on the cavity loss is large, but is suddenly lowered when the Kerr cell is switched off.

Q switching can be effected by using a polarizer and an electro-optical cell, as illustrated in Figure 12.3. The voltage and orientation of the Kerr cell are such that the (linearly polarized) light passing through the polarizer is converted to circularly polarized light. After reflection off the cavity mirror this circularly polarized light is converted by the Kerr cell to light linearly polarized *orthogonally* to the polarizer axis. The presence of the Kerr cell thus prevents feedback, and the cavity is in effect a very lossy one. If the voltage across the Kerr cell is switched off, however, the cell is no longer birefringent. Then the cavity Q has suddenly been increased, and a giant pulse develops.

Saturable Absorbers

Another way of Q switching is to place in the laser cavity a "shutter" consisting of a cell of absorbing material whose absorption coefficient can be saturated (or "bleached") by the laser radiation. Saturation can occur in both absorbing and amplifying media. The absorption (or gain) coefficient decreases with increasing intensity of resonant radiation, becoming nearly zero when the intensity is much larger than a characteristic saturation intensity $I^{\rm sat}$ of the medium (recall Fig. 10.8).

When the gain medium is first pumped, the gain threshold is very high. The cavity loss is too large, because of the absorbing cell, to allow laser oscillation. The medium can therefore be pumped to a high gain without generating significant light intensity. Once the gain is high enough to overcome the loss, however, the cavity intensity grows rapidly. This in turn rapidly saturates the absorption cell, and the effective cavity loss drops abruptly. The whole process leads to a giant-pulse output in a manner similar to that with a mechanical Q switch (Problem 12.4).

The use of a saturable absorber for Q switching is often called *passive* Q switching, in contrast to the *active* Q switching achieved mechanically or electro-optically as described above.

The passive Q switch is obviously simpler in terms of the necessary auxiliary equipment than the two active Q switches we have described. It enjoys an additional advantage: a passive Q switch will often give an output pulse concentrated mostly in a single mode. The reason for this is that it takes a finite time for the

saturable absorber to become highly saturated and thus to raise the cavity Q. In the meantime the cavity intensity originating from spontaneous-emission noise builds up on different modes, and it grows to a greater degree on those modes with the lowest loss per pass. Since a photon can typically make several thousand round trips between the cavity mirrors before the absorber saturates, even small differences in the losses of different modes become significant. The result is that only the lowest-loss mode (or modes) appear in the Q-switched pulse.

In the active Q switches, the switch to high Q is much more rapid, typically occurring during only several tens of photon round trips in the cavity. Small differences in mode losses per pass may then not be sufficient to discriminate among different modes. The output frequency spectrum of a Q-switched ruby laser has long been known to be narrower if a passive Q switch is used instead of a rotating mirror or a Kerr (or Pockels) cell.

12.6 MULTIMODE LASER OSCILLATION

In Section 11.12 we noted that a laser with a homogeneously broadened gain medium tends to oscillate on a single longitudinal mode if the effect of spatial hole burning is small. This expectation is borne out in collision-broadened gas lasers, where atomic motion tends to smear out the effect of spatial hole burning. A similar effect can occur in solid-state lasers in which there is a diffusion of excitation among the atoms. In general, however, oscillation will occur on many longitudinal modes, especially when the gain medium is pumped far above threshold, allowing many modes under the gain curve to meet the threshold condition.

Ruby lasers, for example, are predominantly homogeneously broadened. Due to spatial hole burning, however, they generally oscillate multimode, especially when strongly pumped. As the pumping rate is increased, furthermore, the power associated with any particular mode tends to rise at a slower rate than the total output power on all lasing modes.

Single-longitudinal-mode oscillation is generally precluded by spectral hole burning in inhomogeneously broadened lasers, unless the laser cavity is very short (Figure 11.12) or the pumping rate permits only one mode to reach threshold (Figure 12.4). He-Ne lasers, for example, usually oscillate on several longitudinal

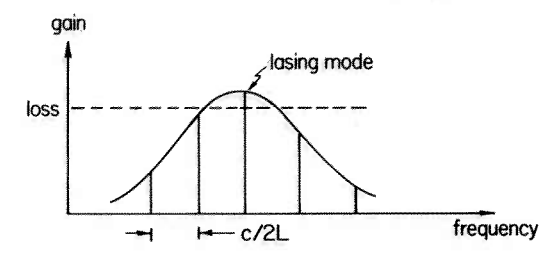


Figure 12.4 A case in which several modes lie under the gain curve, but only one can lase.



Figure 12.5 Typical output spectra of a 1-m-long He-Ne laser for low (a) and high (b) pumping (discharge current) levels.

modes in the absence of any mode selection mechanism (e.g., an etalon). Figure 12.5 shows the output spectrum of a typical, low-pressure, 6328-Å He-Ne laser having a mirror separation L=1 m. Figure 12.5a is the result obtained at a relatively low pumping level. Only one longitudinal mode is above threshold. As the pumping level is raised by increasing the discharge current, however, several modes under the 1700-MHz Doppler profile can oscillate (Figure 12.5b), and their frequency spacing is near c/2L=150 MHz, as expected.

A rigorous theory of laser oscillation must therefore describe the case in which several or many modes oscillate simultaneously. In this case we cannot formulate the theory in terms of a single cavity photon number or intensity. Instead we must specify the photon number or intensity *for each mode*. The analysis is especially complicated by spectral hole burning in the case of inhomogeneous broadening.

The rate equations (10.5.14), or their simplified version (12.2.5b), describe the rate of change of the total number of atoms per unit volume in a particular atomic level. They do not take account of the fact that different atoms may have different line-center frequencies and therefore different stimulated-emission cross sections $\sigma(\nu)$ for radiation of frequency ν . That is, there is no account of inhomogeneous line broadening. If there is inhomogeneous broadening, we must write separate rate equations for different "spectral packets" of atoms. Different spectral packets will then saturate to different degrees (spectral hole burning), and the complications can be enormous in the multimode case. A proper description of this case would, for our purposes, be inordinately lengthy.

In spite of these complexities, there are situations where the gain of a multimode, inhomogeneously broadened laser saturates homogeneously in the sense that every spectral packet saturates in the same manner. In this case a saturation formula like (10.11.4) is applicable, and the total output power on all modes is well described by the Rigrod-type analysis discussed in the preceding chapter. One situation in which this is realized approximately is when the longitudinal mode spacing c/2L is small compared with the homogeneous linewidth $\delta \nu_0$, i.e., when there are many longitudinal modes lying within the frequency interval $\delta \nu_0$. Evidence for the validity of this approximation may be found in the results of experiments with a low-pressure 3.51- μ m He-Xe laser, which is highly inhomogeneously (Doppler) broadened. The cavity mirrors were separated by over 10 m in

order to permit the oscillation of a large number of longitudinal modes. The total output power was described quite well by the Rigrod theory for a *homogeneously* broadened laser. (Section 11.5)

There are other effects tending to "homogenize" the gain saturation. In a gas laser, for instance, collisions will change the z component of an atom's velocity and tend to "fill in" a spectral hole. In other words, collisions act to preserve the Maxwell–Boltzmann velocity distribution, and therefore the Doppler gain profile. Collisions thus act in opposition to the spectral hole-burning effect of the field. At high intensity levels the effective homogeneous linewidth is also increased due to power broadening (Section 10.11).

12.7 PHASE-LOCKED OSCILLATORS

In a Q-switched laser the light pulse must make several passes through the gain medium after the cavity Q is switched. Feedback is necessary in order to build up a large field amplitude by stimulated emission. For some applications it is desirable to have pulses of light even shorter than can be achieved by Q switching. Such powerful, ultrashort pulses of light can be obtained by a technique known as mode locking.

Whereas Q switching may involve either a single mode or many modes, mode locking is a fundamentally multimode phenomenon. Specifically, mode locking involves the "locking" together of the phases of many cavity longitudinal modes. The purpose of this section is to consider a simple analog of a mode-locked laser. We will consider the problem of adding the displacements of N harmonic oscillators with equally spaced frequencies. That is, we consider the sum of

$$x_n(t) = x_0 \sin(\omega_n t + \phi_0) \tag{12.7.1}$$

where

$$\omega_n = \omega_0 + n\Delta,$$

$$n = -\frac{N-1}{2}, -\frac{N-1}{2} + 1, -\frac{N-1}{2} + 2, \dots, \frac{N-1}{2} \quad (12.7.2)$$

In other words, the amplitudes x_0 and phases ϕ_0 of the oscillators are identical, and their frequencies ω_n are equally spaced by Δ and centered at ω_0 , as shown in Figure 12.6. The sum of the displacements (12.7.1) is

$$X(t) = \sum_{n} x_n(t) = \sum_{-(N-1)/2}^{(N-1)/2} x_0 \sin(\omega_n t + \phi_0)$$
 (12.7.3)

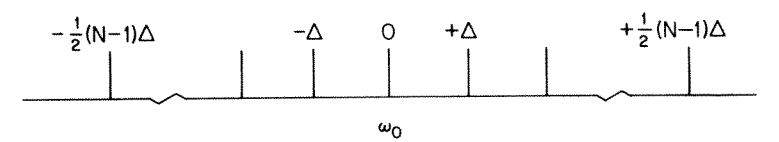


Figure 12.6 A collection of N frequencies running from $\omega_0 - \frac{1}{2}(N-1)\Delta$ to $\omega_0 + \frac{1}{2}(N-1)\Delta$ as in Eq. (12.7.2).

Since $\sin x$ is the imaginary part of e^{ix} , we may write this as

$$X(t) = x_0 \operatorname{Im} \left(\sum_{n} e^{i(\omega_0 t + \phi_0 + n\Delta t)} \right)$$

$$= x_0 \operatorname{Im} \left(e^{i(\omega_0 t + \phi_0)} \sum_{n} e^{in\Delta t} \right)$$
(12.7.4)

The general identity

$$\sum_{-(N-1)/2}^{(N-1)/2} e^{iny} = \frac{\sin(Ny/2)}{\sin(y/2)}$$
 (12.7.5)

proved below allows us to write (12.7.4) as

$$X(t) = x_0 \operatorname{Im} \left(e^{i(\omega_0 t + \phi_0)} \frac{\sin(N\Delta t/2)}{\sin(\Delta t/2)} \right)$$

$$= x_0 \sin(\omega_0 t + \phi_0) \left(\frac{\sin(N\Delta t/2)}{\sin(\Delta t/2)} \right)$$

$$= A_N(t) x_0 \sin(\omega_0 t + \phi_0)$$
(12.7.6)

The function $A_N(t)$ is plotted in Figure 12.7 for N=3 and N=7. In general $A_N(t)$ has equal maxima

$$A_N(t)_{\text{max}} = N \tag{12.7.7}$$

at values of t given by

$$t_m = m\left(\frac{2\pi}{\Delta}\right) \equiv mT, \quad m = 0, \pm 1, \pm 2, \dots$$
 (12.7.8)

As N increases, the maxima of $A_N(t)$ become larger. They also become more

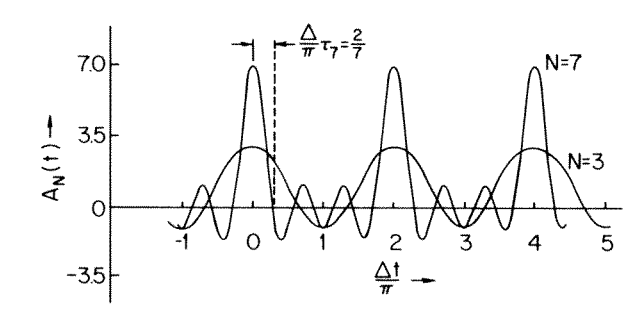


Figure 12.7 The function $A_N(t) = (\sin \frac{1}{2} N \Delta t) / (\sin \frac{1}{2} \Delta t)$ vs. $\Delta t / \pi$.

sharply peaked. A measure of their width is the time interval τ_N indicated in Figure 12.7 for N=7:

$$\tau_N = \frac{2\pi}{N\Delta} = \frac{T}{N} \tag{12.7.9}$$

We have thus shown that the addition of N oscillators of equal amplitudes and phases, and equally spaced frequencies (12.7.2), gives maximum total oscillation amplitudes equal to N times the amplitude of a single oscillator. These maximum amplitudes occur at intervals of time T [Eq. (12.7.8)]. For large N we have, loosely speaking, a series of large-amplitude "spikes." The smaller the frequency spacing Δ between the individual oscillators, the larger the time interval $T = 2\pi/\Delta$ between spikes, and conversely. The temporal duration of each spike is $\tau_N = T/N$, so the spikes get sharper as N is increased.

We have assumed for simplicity that each oscillator has the same phase ϕ_0 [Eq. (12.7.1)]. A more general kind of phase locking occurs when the phase differences of the oscillators are constant but not necessarily zero:

$$\phi_n = \phi_0 + n\alpha \tag{12.7.10a}$$

or

$$\phi_{n+1} - \phi_n = \alpha \tag{12.7.10b}$$

In this case the sum of the oscillator displacements (12.7.3) is replaced by

$$X(t) = \sum_{n} x_0 \sin x_0 (\omega_n t + \phi_n)$$

$$= x_0 \operatorname{Im} \left(e^{i(\omega_0 t + \phi_0)} \sum_{-(1/2)(N-1)}^{(N-1)/2} e^{in(\Delta t + \alpha)} \right)$$
(12.7.11)

and this may be evaluated to give the total displacement

$$X(t) = x_0 \sin(\omega_0 t + \phi_0) \left(\frac{\sin N(\Delta t + \alpha)/2}{\sin(\Delta t + \alpha)/2} \right)$$
(12.7.12)

having basically the same properties as (12.7.6) obtained with $\alpha = 0$. (See also Problem 12.5.)

• We prove (12.7.5) as follows. Let the sum be denoted S_N . For convenience we will first evaluate S_{N+1} .

$$S_{N+1} = \sum_{n=-N/2}^{+N/2} e^{iny}$$
 (12.7.13)

The first step is to shift the summation label by introducing

$$m = n + N/2 \tag{12.7.14}$$

so that

$$S_{N+1} = \sum_{m=0}^{N} e^{i(m-N/2)y}$$

$$= e^{-iNy/2} \sum_{m=0}^{N} e^{imy}$$

$$= e^{-iNy/2} \sum_{m=0}^{N} (e^{iy})^{m}$$
(12.7.15)

The second step is to make use of the identity

$$\sum_{m=0}^{N} x^m = \frac{1 - x^{N+1}}{1 - x} \tag{12.7.16}$$

Then we can write

$$S_{N+1} = e^{-iNy/2} \frac{1 - e^{i(N+1)y}}{1 - e^{iy}}$$

$$= e^{-iNy/2} \frac{e^{i(N+1)y/2}}{e^{iy/2}} \frac{e^{-i(N+1)y/2} - e^{i(N+1)y/2}}{e^{-iy/2} - e^{iy/2}}$$

$$= \frac{\sin(N+1)y/2}{\sin y/2}$$
(12.7.17)

Thus we have proved

$$S_N = \frac{\sin Ny/2}{\sin y/2}$$
 (12.7.18)

as claimed in (12.7.5). •

12.8 MODE LOCKING

What we have in the example of the preceding section is a simple model of a modelocked laser. The individual oscillators in the model play the role of individual longitudinal-mode fields, while their frequency spacing Δ represents the mode (angular) frequency separation $2\pi(c/2L) = \pi c/L$. The assumption of equal oscillator phase differences α ("phase locking") in the model corresponds to the locking together of the phases of the different cavity modes.

Our oscillator model suggests that, if we can somehow manage to lock together the phases of N longitudinal modes of a laser, then the light coming out of the laser will consist of a *train of pulses* separated in time by $T = 2\pi/\Delta = 2L/c$. The temporal duration of each pulse in the train will be $\tau_N = T/N = 2L/cN$. The larger the number N of phase-locked modes, the greater the amplitude, and the shorter the duration, of each individual pulse in the train. As we will see, this is indeed the essence of the mode-locking technique for obtaining ultrashort, powerful laser pulses.

The number of longitudinal modes that can simultaneously lase is determined by the gain linewidth (FWHM) $\Delta \nu_g$ and the frequency separation c/2L between modes (cf. Figure 12.8). Under sufficiently strong pumping of the gain medium we expect that approximately

$$M = \frac{\Delta \nu_g}{c/2L} = \frac{2L}{c} \, \Delta \nu_g \tag{12.8.1}$$

longitudinal modes can oscillate simultaneously. The shortest pulse length we expect to achieve by mode locking is therefore

$$\tau_{\min} = \tau_M = \frac{2L}{cM} = \frac{1}{\Delta \nu_o} \tag{12.8.2}$$

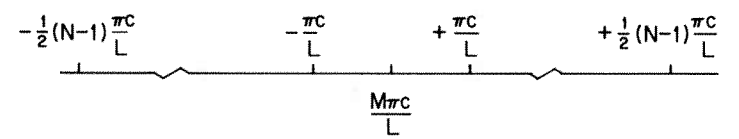


Figure 12.8 The distribution of N cavity mode frequencies as given by Eq. (12.8.7). The situation is exactly the same as in Figure 12.7 for the case of N phase-locked oscillators.

That is, the shortest pulse duration we can achieve by mode locking is (approximately) the reciprocal of the gain linewidth.

As an example, consider the 6328-Å He-Ne laser with a gain linewidth $\Delta \nu_g = \delta \nu_D = 1700$ MHz. For such a laser the shortest pulses obtainable by mode locking are of duration

$$\frac{1}{\delta \nu_D} = \frac{1}{1700 \times 10^6 \text{ sec}^{-1}} \approx 1 \text{ nsec}$$
 (12.8.3)

In other words, for this laser, mode locking is not much of an improvement over Q switching for the production of short pulses. This is often true of gas lasers. Their gain linewidths are so narrow that ultrashort (say, picosecond, 10^{-12} sec duration) pulses cannot be obtained by mode locking.

On the other hand, consider a 6934-Å ruby laser with $\Delta \nu_g \approx 10^{11} \ {\rm sec}^{-1}$. For this laser mode-locked pulses of 10^{-11} sec may be obtained.

Liquid dye lasers typically have broad gain profiles, with $\Delta \nu_g \approx 10^{12}~{\rm sec}^{-1}$ or more. With such lasers mode-locked pulses in the picosecond range are routinely obtained.

A basic understanding of mode-locked laser oscillation may be reached by extending only slightly our analysis of phase-locked oscillators. We associate with the *m*th longitudinal mode an electric field

$$\mathbf{E}_{m}(z, t) = \hat{\mathbf{e}}_{m} \, \mathcal{E}_{m}(z) \, \sin(\omega_{m} t + \phi_{m})$$

$$= \hat{\mathbf{e}}_{m} \, \mathcal{E}_{m} \, \sin k_{m} z \, \sin(\omega_{m} t + \phi_{m}) \qquad (12.8.4)$$

where

$$k_m = m \frac{\pi}{L}, \qquad m = 1, 2, 3, \dots$$
 (12.8.5a)

and

$$\omega_m = k_m c = m \frac{\pi c}{L}, \qquad m = 1, 2, 3, \dots$$
 (12.8.5b)

For simplicity let us assume that the mode fields all have the same magnitude (\mathcal{E}_0) and polarization, so that we can do our calculations below with scalar quantities. Furthermore let us consider, without much loss of generality, the simplest example of phase locking, in which all $\phi_m = 0$. Then the total electric field in the cavity is

$$E(z, t) = \sum_{m} E_{m}(z, t)$$

$$= \mathcal{E}_{0} \sum_{m} \sin k_{m} z \sin \omega_{m} t \qquad (12.8.6)$$

where the summation is over all oscillating modes.

For a cavity 1 m long, $\pi c/L \approx 9 \times 10^8$ Hz. For near-optical frequencies, of course, the lasing frequencies ω_m will be much larger; at a wavelength of 6000 Å, $\omega = 2\pi c/\lambda \approx 3 \times 10^{15}$ Hz. The integer m in (12.8.5) will therefore typically be in the millions. So let us write (12.8.5) as

$$k_m = (M + n) \pi / L \tag{12.8.7a}$$

$$\omega_m = (M+n) \pi c/L \tag{12.8.7b}$$

where M is a very large positive integer $(M \approx 10^6)$ and n runs from $-\frac{1}{2}(N-1)$ to $+\frac{1}{2}(N-1)$, corresponding to a total of N (<< M) modes centered at the frequency $M\pi c/L$ (Figure 12.8). Then (12.8.6) becomes

$$E(z,t) = \mathcal{E}_0 \sum_{-(N-1)/2}^{(N-1)/2} \sin \frac{(M+n)\pi z}{L} \sin \frac{(M+n)\pi ct}{L}$$

$$= \frac{1}{2} \mathcal{E}_0 \sum_{n} \left(\cos \frac{(M+n)\pi (z-ct)}{L} - \cos \frac{(M+n)\pi (z+ct)}{L} \right)$$
(12.8.8)

for the total electric field in the laser cavity.

Now we proceed as in the preceding section. The sum

$$\sum_{-(N-1)/2}^{(N-1)/2} \cos \frac{(M+n) \pi(z-ct)}{L}$$

$$= \operatorname{Re} \sum_{n=-(N-1)/2}^{(N-1)/2} e^{i(M+n)\pi(z-ct)/L}$$

$$= \operatorname{Re} \left(e^{iM\pi(z-ct)/L} \frac{\sin \pi N(z-ct)/2L}{\sin \pi(z-ct)/2L} \right)$$

$$= \left(\cos \frac{M\pi(z-ct)}{L} \right) \frac{\sin \pi N(z-ct)/2L}{\sin \pi(z-ct)/2L}$$
 (12.8.9)

where we have again used the identity (12.7.5). Similarly

$$\sum_{n} \cos \frac{(M+n) \pi(z+ct)}{L} = \left(\cos \frac{M\pi(z+ct)}{L}\right) \frac{\sin \pi N(z+ct)/2L}{\sin \pi(z+ct)/2L}$$
(12.8.10)

From (12.8.8), then,

$$E(z, t) = \frac{\mathcal{E}_0}{2} \left(\cos k_0 (z - ct) \frac{\sin N\pi (z - ct)/2L}{\sin \pi (z - ct)/2L} - \cos k_0 (z + ct) \frac{\sin N\pi (z + ct)/2L}{\sin \pi (z + ct)/2L} \right)$$
(12.8.11)

where $k_0 = \pi M/L$.

The functions

$$A_N^{(\pm)}(z,t) = \frac{\sin N\pi(z \pm ct)/2L}{\sin \pi(z \pm ct)/2L}$$
 (12.8.12)

appearing in (12.8.11) have basically the same form—and effect—as the function $A_N(t)$ appearing in Eq. (12.7.6) for the phase-locked oscillator model. In particular, $A_N^{(\pm)}(z,t)$ has maxima occurring at

$$z \pm ct = m(2L), \quad m = 0, \pm 1, \pm 2, \dots$$
 (12.8.13)

If we put our attention on a fixed value of z inside the cavity, for instance, there are pulses of peak amplitude $N\mathcal{E}_0/2$ appearing at time intervals of 2L/c, each pulse having a duration T/N (Figure 12.9). If we fix our attention on the spatial distribution of E(z,t) at a fixed time t, we find pulses of amplitude $N\mathcal{E}_0/2$ with spatial separation 2L, each pulse having a spatial extent of 2L/N (Figure 12.10).

In other words, the field (12.8.11) represents two trains of pulses, one moving in the positive z direction and the other in the negative z direction. In the usual situation in which output is obtained through one of the cavity mirrors, the laser radiation appears as a single train of pulses of temporal separation and duration 2L/c and 2L/cN, respectively. All this confirms our conclusions deduced from the phase-locked oscillator model.

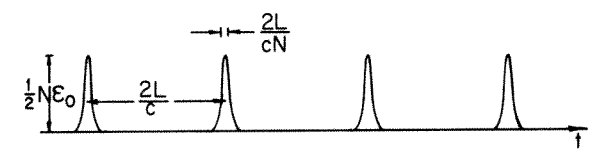


Figure 12.9 A mode-locked pulse train as a function of time, observed at a fixed position z.

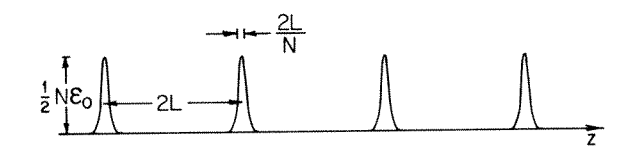


Figure 12.10 A mode-locked pulse train as a function of coordinate z, observed at a fixed instant of time.

The fact that the pulses of a mode-locked train are separated in time by the round-trip cavity transit time 2L/c suggests a "bouncing-ball" picture of a mode-locked laser: we can regard the mode locking as generating a pulse of duration 2L/cN, and this pulse keeps bouncing back and forth between the cavity mirrors. Focusing our attention on a particular plane of constant z in the resonator, we observe a train of identical pulses moving in either direction.

In most lasers the phases ϕ_n of the different modes will undergo random and uncorrelated variations in time. In this case the total intensity is the sum of the individual mode intensities. In mode-locked lasers, however, the mode phases are correlated and the total intensity is not simply the sum of the individual mode intensities. In fact the individual pulses in the mode-locked train have an intensity N times larger than the sum of the individual mode intensities. The average power, however, is essentially unaltered by mode-locking the laser (Problem 12.6).

• Before discussing how mode locking can be accomplished, it is worth noting that "phase locking" or "synchronization" phenomena occur in many *nonlinear* oscillatory systems besides lasers, and indeed these phenomena have been known for a very long time. C. Huygens (1629–1695), for instance, observed that two pendulum clocks hung a few feet apart on a thin wall tend to have their periods synchronized as a result of their small coupling via the vibrations of the wall. Near the end of the nineteenth century Lord Rayleigh found that two organ pipes of slightly different resonance frequencies will vibrate at the same frequency when they are sufficiently close together.

The contractive pulsations of the heart's muscle cells become phase-locked during the development of the fetus. Fibrillation of the heart occurs when they get out of phase for some reason, and results in death unless the heart can be shocked back into the normal condition of cell synchronization. There are other biological examples of phase locking, but detailed theoretical analyses are obviously extremely difficult or impossible for such complex systems. Modern applications of synchronization principles are made in high-precision motors and control systems. •

12.9 AM MODE LOCKING

The process by which phase or mode locking is forced upon a laser is fundamentally a nonlinear one, and a rigorous analysis of it is complicated. We will therefore rely largely on semiquantitative explanations.

Consider again the scalar electric field

$$E_m(z, t) = \mathcal{E}_m \sin k_m z \sin (\omega_m t + \phi_m)$$
 (12.9.1)

associated with a longitudinal mode. Suppose that the amplitude \mathcal{E}_m is not constant but rather is modulated periodically in time according to the formula

$$\mathcal{E}_m = \mathcal{E}_0 (1 + \epsilon \cos \Omega t) \tag{12.9.2}$$

where Ω is the modulation frequency and ε_0 and ϵ are constants. Thus we have an amplitude-modulated field

$$E_m(z,t) = \mathcal{E}_0(1 + \epsilon \cos \Omega t) \sin (\omega_m t + \phi_m) \sin k_m z \qquad (12.9.3)$$

Since

$$\cos \Omega t \sin (\omega_m t + \phi_m) = \frac{1}{2} \sin (\omega_m t + \phi_m + \Omega t) + \frac{1}{2} \sin (\omega_m t + \phi_m - \Omega t)$$
 (12.9.4)

we can write the field (12.9.3) as a sum of harmonically varying parts:

$$E_m(z,t) = \mathcal{E}_0 \left\{ \sin \left(\omega_m t + \phi_m \right) + \frac{\epsilon}{2} \sin \left[(\omega_m + \Omega)t + \phi_m \right] + \frac{\epsilon}{2} \sin \left[(\omega_m - \Omega)t + \phi_m \right] \right\} \sin k_m z$$
 (12.9.5)

The frequency spectrum of the field (12.9.5) is shown in Figure 12.11. The amplitude modulation of the field (12.9.1) of frequency ω_m has generated *side-bands* of frequency $\omega_m \pm \Omega$. These sidebands are displaced from the *carrier frequency* ω_m by precisely the modulation frequency Ω . Sideband generation is a well-known consequence of amplitude modulation.

In a laser the mode amplitudes \mathcal{E}_m are determined by the condition that the gain equals the loss. If the loss (or gain) is periodically modulated at a frequency Ω , we expect the fields $E_m(z,t)$ associated with the various modes to be amplitude-modulated (AM) with this frequency. In other words, we expect sidebands to be generated about each mode frequency ω_m , as in (12.9.5). In particular, if the modulation frequency Ω is equal to the mode frequency spacing

$$\Delta = \omega_{m+1} - \omega_m = \pi c / L \tag{12.9.6}$$

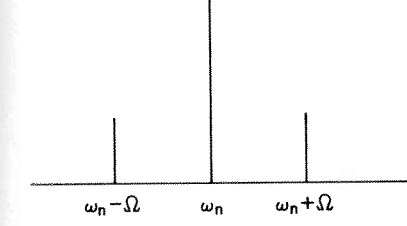


Figure 12.11 Frequency spectrum of the amplitude modulated field (12.9.5). The sidebands at $\omega_n \pm \Omega$ have amplitudes $\epsilon/2$ times as large as the carrier amplitude at ω_n . In this case $\epsilon/2 < 1$.

the sidebands associated with each mode match exactly the frequencies of the two adjacent modes (Figure 12.12). In this case each mode becomes strongly coupled to its nearest-neighbor modes, and it turns out that there is a tendency for the modes to lock together in phase. Loss or gain modulation at the mode separation frequency Δ is therefore one way of mode locking. Borrowing terminology from radio engineering, we call this *AM mode locking*.

The dimensionless factor ϵ appearing in (12.9.2) is called the modulation index. It is usually small, but it must be large enough to couple the different modes sufficiently strongly. This is analogous to the synchronization phenomenon observed in the 17th century by Huygens with pendulum clocks. Their frequencies were locked together when the clocks were mounted just a meter or so apart, but larger separations weakened their coupling and destroyed the locking effect. If ϵ is too large, on the other hand, the locking effect is also weakened. This is analogous to the distortion arising in AM radio electronic systems when the carrier wave is "overmodulated," i.e., when $\epsilon > 1$. (See also Problem 12.7.)

A heuristic way to understand why AM mode locking occurs in lasers is first to suppose that lasing can occur only in brief intervals when the periodically modulated loss is at a minimum. These minima occur in time intervals of $T=2\pi/\Delta=2L/c$ if the modulation frequency $\Omega=\Delta$. Between these times of minimum loss the loss is too large for laser oscillation. Thus we can have laser oscillation only if it is possible to generate a train of short pulses separated in time by T. This is possible if the modes lock together and act in unison, for then we generate a mode-locked train of pulses separated by time T. Thus mode locking has been described as a kind of "survival of the fittest" phenomenon.

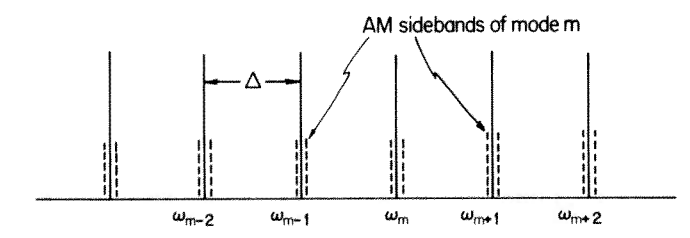


Figure 12.12 Longitudinal modes amplitude-modulated at the frequency Δ equal to their spacing. For clarity the AM sidebands are indicated as dashed lines slightly dispaced from the mode frequencies ω_m .

12.10 FM MODE LOCKING

We will now consider the case where the *phase* of the field (12.9.1) is periodically modulated rather than the amplitude:

$$E_m(z,t) = \mathcal{E}_m \sin k_m z \sin (\omega_m t + \phi_m + \delta \cos \Omega t) \qquad (12.10.1)$$

The dimensionless constant δ gives the amplitude of the modulation of frequency Ω . As in the case of amplitude modulation, this phase modulation gives rise to sideband frequencies about the carrier frequency ω_m . As we will now see, however, the phase modulation produces a whole series of sidebands.

The time-dependent part of (12.10.1) may be written as

$$\sin (\omega_m t + \phi_m + \delta \cos \Omega t) = \sin (\omega_m t + \phi_m) \cos (\delta \cos \Omega t) + \cos (\omega_m t + \phi_m) \sin (\delta \cos \Omega t)$$
(12.10.2)

Now we make use of two mathematical identities:²

$$\cos(x\cos\theta) = J_0(x) + 2\sum_{k=1}^{\infty} (-1)^k J_{2k}(x)\cos(2k\theta) \quad (12.10.3a)$$

and

$$\sin(x\cos\theta) = 2\sum_{k=0}^{\infty} (-1)^k J_{2k+1}(x)\cos[(2k+1)\theta] \quad (12.10.3b)$$

where $J_n(x)$ is the Bessel function of the first kind of order n. The first few lowest-order Bessel functions are plotted in Figure 12.13. These plots are all we will need

2. See, for example M. Abramowitz and I. A. Stegun, *Handbook of Mathematical Functions* (Dover, New York, 1971), formulas 9.1.44 and 9.1.45.

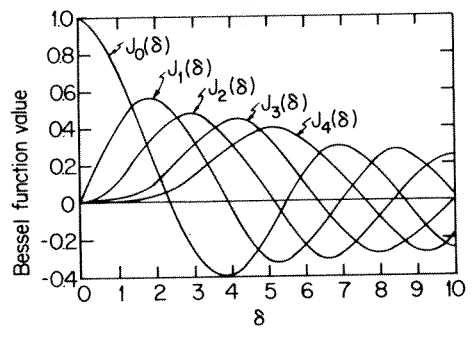


Figure 12.13 The first few lowest-order Bessel functions of the first kind, $J_n(\delta)$.

to know about them. The functions (12.10.3) appear in (12.10.2) with $x = \delta$ and $\theta = \Omega t$. Thus

$$\sin(\omega_{m}t + \phi_{m} + \delta\cos\Omega t)$$

$$= \sin(\omega_{m}t + \phi_{m}) \left(J_{0}(\delta) + 2\sum_{k=1}^{\infty} (-1)^{k} J_{2k}(\delta)\cos(2k\Omega t)\right)$$

$$+ 2\cos(\omega_{m}t + \phi_{m})\sum_{k=0}^{\infty} (-1)^{k} J_{2k+1}(\delta)\cos\left[(2k+1)\Omega t\right]$$

$$= \sin(\omega_{m}t + \phi_{m})\left[J_{0}(\delta) - 2J_{2}(\delta)\cos 2\Omega t\right]$$

$$+ J_{4}(\delta)\cos 4\Omega t - 2J_{6}(\delta)\cos 6\Omega t + \cdots\right]$$

$$+ 2\cos(\omega_{m}t + \phi_{m})\left[J_{1}(\delta)\cos \Omega t - J_{3}(\delta)\cos 3\Omega t\right]$$

$$+ J_{5}(\delta)\cos 5\Omega t - \ldots\right]$$
(12.10.4)

Using the identities

$$\sin x \cos y = \frac{1}{2} \left[\sin (x + y) + \sin (x - y) \right]$$
$$\cos x \cos y = \frac{1}{2} \left[\cos (x + y) + \cos (x - y) \right]$$

therefore, we have

$$\sin (\omega_{m}t + \phi_{m} + \delta \cos \Omega t)$$

$$= J_{0}(\delta) \sin (\omega_{m}t + \phi_{m})$$

$$+ J_{1}(\delta) \left\{ \cos \left[(\omega_{m} + \Omega) t + \phi_{m} \right] + \cos \left[(\omega_{m} - \Omega) t + \phi_{m} \right] \right\}$$

$$- J_{2}(\delta) \left\{ \sin \left[(\omega_{m} + 2\Omega) t + \phi_{m} \right] + \sin \left[(\omega_{m} - 2\Omega) t + \phi_{m} \right] \right\}$$

$$- J_{3}(\delta) \left\{ \cos \left[(\omega_{m} + 3\Omega) t + \phi_{m} \right] + \cos \left[(\omega_{m} - 3\Omega) t + \phi_{m} \right] \right\}$$

$$+ J_{4}(\delta) \left\{ \sin \left[(\omega_{m} + 4\Omega) t + \phi_{m} \right] + \sin \left[(\omega_{m} - 4\Omega) t + \phi_{m} \right] \right\}$$

$$+ J_{5}(\delta) \left\{ \cos \left[(\omega_{m} + 5\Omega) t + \phi_{m} \right] + \cos \left[(\omega_{m} - 5\Omega) t + \phi_{m} \right] \right\}$$

$$- \dots$$

$$(12.10.5)$$

after a simple rearrangement of terms in (12.10.4).

Whereas amplitude modulation produces one sideband on either side of the carrier frequency ω_m , phase modulation in general produces a whole series of pairs of sidebands. If the "modulation index" δ is somewhat less than unity, however, we observe from (12.10.5) and Figure 12.13 that the first pair of sidebands



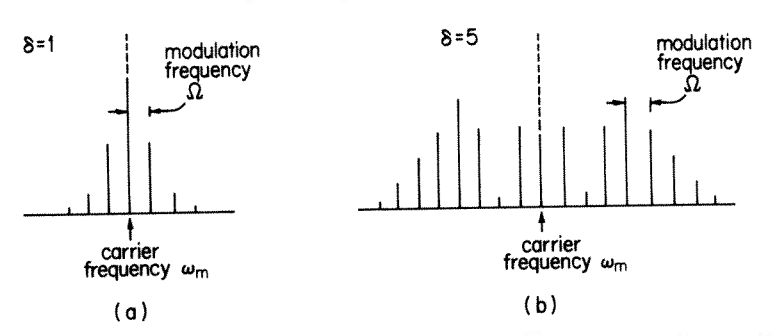


Figure 12.14 Frequency spectrum of the function (12.10.5) for the modulation index (a) $\delta = 1$ and (b) $\delta = 5$.

at $\omega_m \pm \Omega$ is strongest. As the strength of the modulation increases, i.e., as δ increases, more sideband pairs become important. Figure 12.14 shows the frequency spectrum of the function (12.10.5) for $\delta = 1$ and $\delta = 5$.

Again borrowing the terminology of radio engineering, we refer to this type of modulation as frequency modulation (FM). As in the AM case, frequency modulation at the mode separation frequency $\Omega = \Delta = \pi c/L$ causes the sidebands associated with each mode to be in resonance with the carrier frequencies of other modes. This results in a strong coupling of these modes and a tendency for them to lock together and produce a mode-locked train of pulses. This is called FM mode locking.

• Information cannot be transmitted with a purely monochromatic wave. The basic idea of radio communication is to modulate a monochromatic (carrier) wave in some way (AM or FM), transmit it, then demodulate it at a receiver to recover the information contained in the original modulation. In the AM case the sidebands imposed on the carrier wave are displaced from the carrier by an amount equal to the modulation frequency, independently of the modulation index ϵ . In the FM case, on the other hand, the "width" of the modulation about the carrier is directly proportional to the corresponding index δ , approximately independently of the modulation frequency Ω . This makes FM transmission less susceptible to interference from extraneous sources (lightning, electric power generators, etc.) than AM if its modulation index is large. At the same time, there is a disadvantage to FM in that the amplifiers in the transmitter and receiver must have large bandwidths in order to pick up a good portion of the sideband spectrum. A large bandwidth is most easily obtained at higher carrier frequencies; this is analogous to the fact that the bandwidth of a laser cavity increases with frequency if the cavity Q is held constant [Eq. (11.9.21)], and explains why FM radio stations broadcast at higher frequencies than AM stations (Problem 2.9).

12.11 METHODS OF MODE LOCKING

Lasers can be mode-locked in a variety of ways. We will focus our attention on three common and illustrative techniques.

Acoustic Loss Modulation

This method is based on the diffraction of light by sound waves, i.e., on Brillouin scattering. A sound wave is basically a wave of density variation—and therefore refractive index variation (recall Section 2.4)—in a material medium. As discussed in Appendix 12.B, a sound wave can therefore act as a "diffraction grating" for light. A sound wave of wavelength λ_s diffracts light of wavelength λ with diffraction angle θ (Figure 12.19) satisfying (Eq. 12.B.3)

$$\sin \theta = \frac{\lambda}{2n\lambda_s} \tag{12.11.1}$$

where n is the refractive index of the medium.

A standing sound wave in a medium may be represented by a refractive index variation of the form

$$\Delta n(x, t) = a \sin(\omega_s t + \theta) \sin k_s x \qquad (12.11.2)$$

The periodic spatial modulation $\sin k_s x$ of the refractive index gives rise to diffraction at the angle θ given by (12.11.1) with $\lambda_s = 2\pi/k_s$. The temporal oscillation at frequency ω_s means that the diffraction is most effective at times t such that $\sin (\omega_s t + \theta) = \pm 1$, for at these times the "diffraction grating" represented by $\sin k_s x$ has its largest amplitude $(\pm a)$. Thus the diffracting strength of the standing acoustic wave varies harmonically in time with frequency $2\omega_s$.

We can now understand how the diffraction of light by sound can be used to periodically modulate the cavity loss in a laser, and thereby to achieve AM mode locking. If a block of material having a standing acoustic wave is inside the cavity, the diffractive loss associated with it will oscillate with frequency $2\omega_s$. If $2\omega_s = \Delta = \pi c/L$, the cavity loss is modulated at the mode frequency separation, as desired for mode locking. Since audible sound waves have frequencies roughly from 20 Hz to 2×10^4 Hz, while the mode separations in a laser are typically much larger, it is clear that ultrasonic acoustic modulation is required for mode locking. This may be done by driving a block of quartz with a piezoelectric crystal.

Electro-optical Phase Modulation

This method is based on the electro-optical effect. Consider a linearly polarized monochromatic wave propagating in the z direction in a medium with refractive index n:

$$\mathbf{E}(z, t) = \mathbf{\hat{x}} \mathcal{E}_0 \cos(\omega t - kz) = \mathbf{\hat{x}} \mathcal{E}_0 \cos\omega \left(t - \frac{n}{c}z\right) \quad (12.11.3)$$

Suppose we have a Pockels-type electro-optical medium in which the refractive

$$n = n_0 + \beta E_a \tag{12.11.4}$$

Therefore the electric field (12.11.3) in such an electro-optical medium in which an external field E_a is applied is

$$\mathbf{E}(z, t) = \hat{\mathbf{x}} \mathcal{E}_0 \cos \left(\omega t - \frac{n_0 \omega}{c} z - \frac{\beta \omega}{c} E_a z \right)$$
$$= \hat{\mathbf{x}} \mathcal{E}_0 \cos \left[\omega \left(t - \frac{n_0}{c} z \right) - \phi \right]$$
(12.11.5)

where

$$\phi = \frac{\beta \omega}{c} E_a z \tag{12.11.6}$$

After a distance l of propagation in the medium the field has the phase

$$\phi = \frac{\beta\omega}{c} V \tag{12.11.7}$$

where $V = E_a l$ is the potential difference due to the field E_a . Thus if an electrooptical cell is inserted in a laser cavity, the laser can be FM mode-locked by varying the applied voltage V sinusoidally at the mode separation frequency Δ .

In general a linearly polarized electric field entering an electro-optical medium can be decomposed into two orthogonally polarized components, each of which has a different refractive index. The two orthogonal polarization directions are determined by the orientation of the cell and the applied field E_a . In deriving (12.11.7) we have assumed that the incident field is linearly polarized along one of these directions. In the general case the field will have components in both directions, and in a Pockels cell the two components will have different values of β . This results in a phase difference between the two field components. If the cell produces a total phase change of 90°, for example, the incident linearly polarized field will be converted to a circularly polarized field, as in the case illustrated in Figure 12.3 for a Kerr cell. That is, a cell containing an electro-optical material can act as a quarter-wave plate. The advantage of using electro-optical media rather than naturally birefringent materials, of course, is the switching and control capabilities one has through the adjustment of the bias voltage.

Saturable Absorbers

As in the case of Q switching, a "passive" AM mode locking may be achieved through the use of a saturable absorber. Assume for simplicity that the absorption coefficient a of the absorption cell saturates according to the formula

$$a = \frac{a_0}{1 + I/I^{\text{sat}}} \tag{12.11.8}$$

for a homogeneously broadened line. It is also convenient (but not necessary) to assume that the saturation intensity I^{sat} of the absorption line is very large compared with the laser intensity I. Then (12.11.8) is approximated by

$$a \approx a_0 - a_0 I / I^{\text{sat}}$$
 (12.11.9)

Suppose first that there are two oscillating cavity modes, so that the total cavity electric field is

$$E(z, t) = \mathcal{E}_1 \sin k_1 z \sin(\omega_1 t + \phi_1) + \mathcal{E}_2 \sin k_2 z \sin(\omega_2 t + \phi_2) \quad (12.11.10)$$

and the cavity intensity is

$$I(z, t) = c \epsilon_0 E(z, t)^2$$

$$= c \epsilon_0 \left\{ \mathcal{E}_1^2 \sin^2 k_1 z \sin^2 (\omega_1 t + \phi_1) + \mathcal{E}_2^2 \sin^2 k_2 z \sin^2 (\omega_2 t + \phi_2) + 2 \mathcal{E}_1 \mathcal{E}_2 \sin k_1 z \sin k_2 z \sin (\omega_1 t + \phi_1) \sin (\omega_2 t + \phi_2) \right\}$$
(12.11.11)

Now the last term can be rewritten using the identity

$$2 \sin(\omega_1 t + \phi_1) \sin(\omega_2 t + \phi_2) = \cos[(\omega_1 - \omega_2)t + \phi_1 - \phi_2] - \cos[(\omega_1 + \omega_2)t + \phi_1 + \phi_2]$$
(12.11.12)

The frequencies ω_1 , ω_2 , and $\omega_1 + \omega_2$ are very large compared with the mode separation frequency $\omega_1 - \omega_2 = \Delta$. If we average the intensity (12.11.11) over a few optical periods, therefore, we obtain

$$\bar{I}(z,t) = \frac{c\epsilon_0}{2} \left[\mathcal{E}_1^2 \sin^2 k_1 z + \mathcal{E}_2^2 \sin^2 k_2 z + 2\mathcal{E}_1 \mathcal{E}_2 \sin k_1 z \sin k_2 z \cos(\Delta t + \phi_1 - \phi_2) \right]$$
(12.11.13)

The intensity \overline{I} has a time dependence that is simply a sinusoidal oscillation at the mode beat frequency Δ . The absorption coefficient (12.11.9) averaged over a few optical periods will therefore have this same time dependence. In other words, if a saturable absorber described by (12.11.8) is placed inside the laser cavity, it results in a cavity loss modulated at the mode separation frequency, and therefore acts to mode-lock the laser. The argument may be extended to the case of N cavity modes, and we conclude that mode-locked operation may be achieved by placing a cell containing a saturable absorber inside the cavity.

This technique is commonly used in mode-locked solid-state and dye lasers, which, as discussed in Section 12.8, are especially attractive in this regard.

• Although both Q switching and mode locking may be accomplished by inserting a cell containing a saturable absorber into the laser cavity, there are somewhat different requirements for the absorber in the two cases.

In the case of mode locking the absorber should respond very quickly to any changes in the cavity intensity. This was implied in our discussion above, where it was assumed that the saturation behavior of the absorber is fixed according to (12.11.8); there are no transient terms showing how a changes from $a_0(1 + I_1/I^{\text{sat}})^{-1}$ to $a_0(1 + I_2/I^{\text{sat}})^{-1}$ as I changes from I_1 to I_2 . Rather, it was assumed that a reacts instantaneously to variations in I, or at least with a response time shorter than 2L/c. This requires the absorber to have a short relaxation time, whereas a longer one would be tolerable for Q switching.

Similarly, it is desirable for Q switching that the saturation intensity of the absorber be considerably smaller than that of the laser gain medium. This ensures a large, unsaturated gain after the loss associated with the absorption cell is fully saturated, and allows the giant pulse to build up. In the case of mode locking, however, a relatively large absorber saturation intensity can still give rise to the required modulation. Our assumption $I \ll I^{\text{sat}}$ in (12.11.9) was made for convenience, not necessity.

Thus it is possible to Q-switch a laser with one absorption cell and mode-lock it with another. Frequently, however, both effects are present with a saturable absorber, and a Q-switched laser will show signs of mode locking. The output of such a Q-switched, mode-locked laser is indicated in Figure 12.15. \bullet

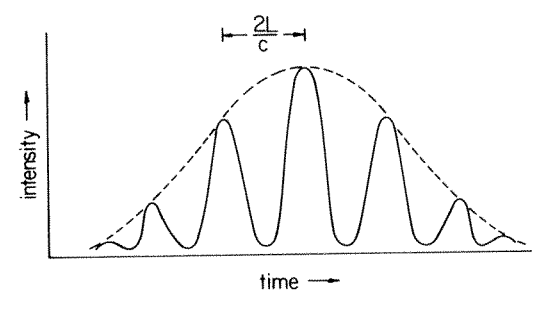


Figure 12.15 Output intensity vs. time of a Q-switched, mode-locked laser. The dashed curve is the envelope of the mode-locked pulse train. Each contributing mode viewed individually has the time dependence of the Q-switched envelope, but because the modes are locked the total output is in the form of a group of pulses separated in time by 2L/c.

12.12 AMPLIFICATION OF SHORT OPTICAL PULSES

In many applications it is necessary to amplify laser radiation by passing it through a medium with a population inversion on a resonant transition. The amplifier is often made of the same material, and pumped in the same way, as the gain cell of the laser. The most important difference between the laser and the amplifier is simply that the amplifier does not have a resonator with mirrors for feedback. Radiation incident on the amplifier undergoes amplification by stimulated emission and emerges at the other end with greater energy. A series of amplifiers may be employed in tandem, and mirrors may be used to allow the beam to make several passes through a single amplifier. In this section we will consider a pulse of radiation making a single pass through an amplifier.

We will assume that the duration of the laser pulse is short compared with any pumping or relaxation times, so that the changes in level populations in the amplifier are due mainly to stimulated emission and absorption. The rate equations for the level population densities of the amplifying transition are then simply

$$\frac{\partial N_2}{\partial t} = -\frac{\sigma}{h\nu} \left(N_2 - N_1 \right) I \tag{12.12.1a}$$

$$\frac{\partial N_1}{\partial t} = \frac{\sigma}{h\nu} \left(N_2 - N_1 \right) I \tag{12.12.1b}$$

since pumping and relaxation processes do not affect N_2 and N_1 significantly during the pulse; this condition for a "short" pulse typically requires pulse lengths shorter than about a nanosecond. Equations (12.12.1) may be combined to form a single equation for the population difference $N \equiv N_2 - N_1$:

$$\frac{\partial N}{\partial t} = -\frac{2\sigma}{h\nu}NI \tag{12.12.2}$$

We also write the (plane-wave) equation for the variation in space and time of the intensity:

$$\frac{\partial I}{\partial z} + \frac{1}{c} \frac{\partial I}{\partial t} = \sigma N I \tag{12.12.3}$$

Let us integrate both sides of (12.12.3) over time:

$$\int_{-\infty}^{\infty} \left(\frac{\partial I}{\partial z} + \frac{1}{c} \frac{\partial I}{\partial t} \right) dt = \int_{-\infty}^{\infty} \sigma N I \, dt \qquad (12.12.4)$$

Here $t = -\infty$ and $t = +\infty$ denote times long before and after the pulse has "turned on" at z, so that $I(z, t = -\infty) = I(z, t = +\infty) = 0$. Thus

 $\int_{-\infty}^{\infty} \frac{\partial I}{\partial t} dt = I(z, t = +\infty) - I(z, t = -\infty) = 0$ (12.12.5)

and so (12.12.4) becomes

$$\frac{d\phi}{dz} = \sigma \int_{-\infty}^{\infty} N(z, t) I(z, t) dt \qquad (12.12.6)$$

where

$$\phi(z) \equiv \int_{-\infty}^{\infty} I(z, t) dt \qquad (12.12.7)$$

is called the *fluence*, and is a measure of the total energy content of the pulse. Note that the fluence has units of energy per unit area, and should not be confused with the photon flux Φ (number of photons per unit area and time) that was introduced in Chapter 7 and used extensively in Chapter 10.

Equation (12.12.6) may be simplified by solving (12.12.2) for N(z, t):

$$N(z, t) = N(z, -\infty) \exp\left(-\frac{2\sigma}{h\nu} \int_{-\infty}^{t} I(z, t') dt'\right) \qquad (12.12.8)$$

where $N(z, -\infty)$ is the population inversion at z before the pulse has arrived. Thus we find

$$\frac{d\phi}{dz} = \sigma N(z, -\infty) \int_{-\infty}^{\infty} I(z, t) \exp\left(-\frac{2\sigma}{h\nu} \int_{-\infty}^{t} I(z, t') dt'\right) dt$$

$$= -\sigma N(z, -\infty) \int_{-\infty}^{\infty} \frac{h\nu}{2\sigma} \frac{\partial}{\partial t} \left[\exp\left(-\frac{2\sigma}{h\nu} \int_{-\infty}^{t} I(z, t') dt'\right) \right] dt$$

$$= -\frac{h\nu}{2} N(z, -\infty) \left[\exp\left(-\frac{2\sigma}{h\nu} \int_{-\infty}^{\infty} I(z, t) dt\right) - 1 \right] \qquad (12.12.9)$$

Then use of (12.12.7) allows us to write

$$\frac{d\phi}{dz} = \frac{h\nu}{2} N(z, -\infty) \left[1 - \exp\left(-\frac{2\sigma\phi(z)}{h\nu}\right) \right]
= \frac{h\nu}{2} N(z, -\infty) \left[1 - \exp\left(-\frac{\phi(z)}{\phi_{\text{sat}}}\right) \right]$$
(12.12.10)

where we define the saturation fluence

$$\phi_{\text{sat}} \equiv h\nu/2\sigma \tag{12.12.11}$$

This is just the photon energy divided by twice the stimulated-emission cross section.

The differential equation (12.12.10) may be written in terms of the ratio $\theta(z) = \phi(z)/\phi_{\text{sat}}$:

$$\frac{d\theta}{dz} = g_0(1 - e^{-\theta}) \tag{12.12.12}$$

where we have used the fact that the small-signal gain coefficient $g_0(z, -\infty) = \sigma N(z, -\infty)$. In many cases of interest the spatial variations of g_0 are small, and we can take g_0 to be a constant in the differential equation (12.12.12) for the fluence. Then this equation has the solution

$$\theta(z) = \ln\left[1 + e^{g_0 z} (e^{\theta(0)} - 1)\right] \tag{12.12.13}$$

or

$$\phi_{\text{out}} = \phi_{\text{sat}} \ln \left[1 + G_0 \left(\exp \left(\phi_{\text{in}} / \phi_{\text{sat}} \right) - 1 \right) \right]$$
 (12.12.14)

where $\phi_{\text{out}} \equiv \phi(L)$ is the output fluence of an amplifier of length L with small-signal total gain $G_0 = e^{g_0 L}$, given the input fluence $\phi_{\text{in}} = \phi(0)$ to the amplifier. We can also write (12.12.14) in terms of the total gain $G \equiv \phi_{\text{out}}/\phi_{\text{in}}$:

$$G = \frac{\phi_{\text{out}}}{\phi_{\text{in}}} = X^{-1} \ln \left[1 + G_0(e^X - 1) \right], \quad X = \frac{\phi_{\text{in}}}{\phi_{\text{sat}}} \quad (12.12.15)$$

It is important to note that this solution for the output fluence is independent of the shape of the pulse as a function of time. As long as the pulse is confined, to a good approximation, to a finite duration, and this duration is short compared with any pumping and relaxation times, Eq. (12.12.15) gives us the output fluence as a function of the small-signal gain, length, and saturation fluence of the amplifier. In Figure 12.16 we plot G as a function of X, assuming a small-signal total gain factor $G_0 = 5000$.

If $X = \phi_{in}/\phi_{sat} << 1$, then (12.12.15) becomes

$$G \approx X^{-1} \ln (1 + G_0 X)$$
 (12.12.16)

If furthermore $G_0X << 1$, then $\ln (1 + G_0X) \approx G_0X$ and we have the small-signal limit on total gain

$$G \approx G_0 = e^{g_0 L} {(12.12.17)}$$

If $e^{X} = \exp(\phi_{in}/\phi_{sat}) >> 1$, on the other hand, then

$$G \approx X^{-1} \ln (G_0 e^X) = X^{-1} \ln (\exp (g_0 L + X))$$

= $X^{-1} (g_0 L + X) = 1 + g_0 L/X$ (12.12.18a)

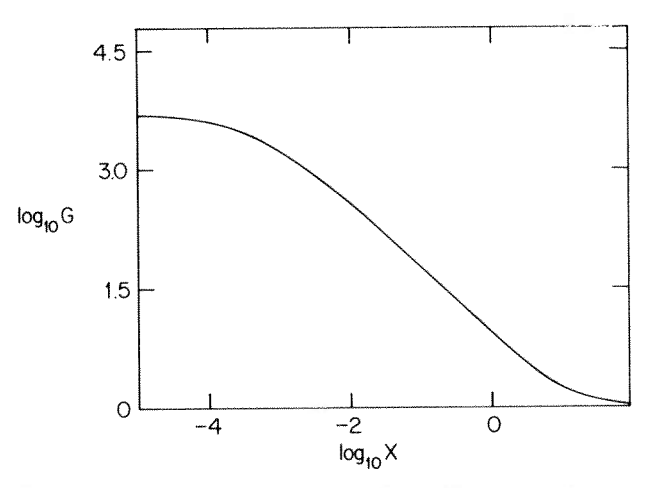


Figure 12.16 Gain G(X) [Eq. (12.12.15)] for $G_0 = 5000$.

or

$$\phi_{\text{out}} \approx \phi_{\text{in}} + (g_0 \phi_{\text{sat}}) L \qquad (12.12.18b)$$

This result identifies $g_0\phi_{\rm sat}$ as the largest energy per unit volume that can be extracted from the amplifier when $\phi_{\rm in}$ is large compared with $\phi_{\rm sat}$. This is analogous to the result (11.3.8) for a cw laser, where $g_0I_{\rm sat}$ is the largest possible rate of energy extraction per unit volume. Using the fact that $g_0 = \sigma N$ and $\phi_{\rm sat} = h\nu/2\sigma$, we can write (12.12.18) in the form

$$\phi_{\text{out}} \approx \phi_{\text{in}} + \frac{Nh\nu}{2}L \qquad (12.12.19)$$

This says that the largest extractable energy density corresponds to taking half a photon, on average, from each excited atom of the amplifier. The reason for the factor $\frac{1}{2}$ is simply that in the limit of large $\phi_{\rm in}/\phi_{\rm sat}$ under consideration, the amplifier is well saturated, with the upper- and lower-level populations having equal probabilities.

This theory of short-pulse amplification is often referred to as the *Frantz-Nod-vik model*,³ and is useful in the design and interpretation of short-pulse amplification experiments. It is worth noting, however, that the model, which is based on the rate-equation approximation, does not account for coherent effects like 2π -pulse formation (Section 8.2 and Problem 8.4).

3. L. M. Frantz and J. S. Nodvik, Journal of Applied Physics 24, 2346 (1963).

12.13 AMPLIFIED SPONTANEOUS EMISSION

The theory of pulse propagation presented in the preceding section is used frequently in the analysis of laser amplifiers. However, for high-gain systems this theory ignores an important phenomenon: the amplifier can amplify not only the input field from a laser oscillator (or another amplifier), but also the spontaneous radiation emitted by the excited molecules of the amplifier itself. It is easy to see that spontaneously emitted photons at one end of an amplifier, which happen to be directed along the amplifier axis, or close to that direction, can *stimulate* the emission of more photons and lead to substantial output radiation at the other end of the amplifier. This radiation, which appears regardless of whether there is any input radiation, is called *amplified spontaneous emission* (ASE).

It is clear that ASE will have at least some properties resembling laser radiation. In particular, it will be narrow-band in frequency and it will also be highly directional, simply because the amplifier is long and thin. For these reasons high-gain systems emitting ASE are often referred to as "mirrorless lasers." Such mirrorless lasing, also called "superradiance," is well known in the 3.39 μ m He-Ne laser, and in high-gain excimer, dye, and semiconductor laser media.

For a simple quantitative description of ASE, let us consider the steady-state equation for the propagation of intensity in an amplifying medium characterized by the gain coefficient g, namely

$$\frac{dI}{dz} = gI \tag{12.13.1}$$

If I(0) = 0, then this equation predicts that I(z) = 0 for all z. In other words, this equation does not account for ASE. To include the possibility of ASE we add to (12.13.1) the effect of spontaneous emission:

$$\frac{dI}{dz} = gI + (A_{21}N_2h\nu)(\Omega/4\pi)$$
 (12.13.2)

The added term is the contribution to dI/dz from spontaneous emission of photons of energy $h\nu$ by N_2 excited molecules per unit volume with spontaneous emission rate A_{21} . Since spontaneous emission is (statistically) isotropic, we have included a factor $\Omega/4\pi$, where Ω is an appropriate solid angle; this factor accounts for the fact that only a fraction $\Omega/4\pi$ of spontaneously emitted photons are emitted in directions for which amplification can occur. In the simplest approximation Ω is taken to be A/L^2 , where A is the cross-sectional area of the amplifier and L is its length.

In the small-signal regime in which g and N_2 are independent of I, we have the following solution of equation (12.13.2):

for $\exp(gz) >> 1$. For simplicity we will assume that the lower-level population of the amplifying transition is negligible, so that $g \cong \sigma N_2$, where σ is the stimulated emission cross section. For a homogeneously broadened transition having a Lorentzian lineshape of full width at half-maximum $\Delta \nu$ we have

$$\sigma = \left(\frac{\lambda^2 A_{21}}{8\pi}\right) \left(\frac{2}{\pi \Delta \nu}\right) = \frac{\lambda^4 A_{21}}{4\pi^2 c \Delta \lambda} \tag{12.13.4}$$

where $\Delta \lambda = (c/\nu^2)\Delta \nu$ is the width in the emission wavelength $\lambda = c/\nu$. In this case (12.13.3) becomes

$$I(z) \approx \left(\frac{\pi h c^2 \Omega}{\lambda^5}\right) \Delta \lambda e^{gz}$$
 (12.13.5)

for the growth of intensity with propagation in the amplifier.

The result (12.13.5) allows us to estimate the importance of ASE in high-gain amplifiers. [In careful design analyses, of course, it is necessary to include gain saturation, which has not been done in the derivation of (12.13.5).] ASE can be detrimental to the performance of amplifier systems for two reasons. First, the ASE can significantly deplete the upper-level population, thus diminishing the gain available to the input signal to be amplified. Second, the ASE radiation can irradiate a target before the arrival of the amplified signal, and thus modify an experiment in unintended ways.

ASE can be expected to deplete seriously the upper-level population of the amplifying transition if it becomes comparable in magnitude to the saturation intensity, I^{sat} , of the transition. Setting I(L) given by (12.13.5) equal to I^{sat} , we have

$$gL = \log \left[\frac{\lambda^5 I^{\text{sat}}}{\pi h c^2 \Omega \Delta \lambda} \right]$$
 (12.13.6)

for the gain-length product of the amplifier at which gain depletion due to ASE may be an important consideration. It is clear from this formula (and (12.13.5)) that large-bore amplifiers, subtending large solid angles, are most susceptible to ASE problems.

• Amplified spontaneous emission is sometimes described from the standpoint of an "effective noise input." This approach is based on (12.13.1) rather than (12.13.2). It begins by noting that, since equation (12.13.1) gives I(z) = 0 for all z if I(0) = 0, some effective

input $I(0) = I_{\rm eff} \neq 0$ is necessary in order to obtain a nonvanishing I(z). An expression for $I_{\rm eff}$ is obtained by recalling that in a cavity of dimensions large compared with a wavelength there are $(8\pi \nu^2/c^3)\Delta\nu$ modes of the field per unit volume in the frequency interval $[\nu, \nu + \Delta\nu]$. (Section 1.3) And according to the quantum theory of radiation each of these modes has a zero-point energy $\frac{1}{2}h\nu$. There is therefore a zero-point field energy per unit volume

$$\rho_o(\nu) = \left(\frac{8\pi\nu^2}{c^3}\right)^{1/2} h\nu\Delta\nu = \left(\frac{4\pi h\nu^3}{c^3}\right) \frac{c\Delta\lambda}{\lambda^2}$$
 (12.13.7)

in the wavelength interval $[\lambda, \lambda + \Delta \lambda]$. Clearly we should take $\Delta \lambda$ to be on the order of the spectral width of the laser transition. For our purposes we replace $\Delta \lambda$ in (12.13.7) by $\pi \Delta \lambda$, where $\Delta \lambda$ is the transition linewidth (FWHM). Then the "quantum noise" intensity at the laser transition wavelength λ is given by

$$I_{\text{eff}} = c\rho_o(\nu)\Omega/4\pi = \left(\frac{\pi hc^2\Omega}{\lambda^5}\right)\Delta\lambda$$
 (12.13.8)

where we have inserted the factor $\Omega/4\pi$ to account for the fact that only those modes within the solid angle Ω appropriate to the amplifier can act as effective noise sources. Thus, from (12.13.1),

$$I(z) = I_{\text{eff}} e^{gz} = \left(\frac{\pi h c^2 \Omega}{\lambda^5}\right) \Delta \lambda e^{gz}$$
 (12.13.9)

which reproduces (12.13.5), and thus validates the approach to ASE based on an effective noise input. \bullet

ASE radiation can have spatial coherence comparable to true laser radiation, but it generally lacks the same degree of temporal coherence. (See Chapter 15 for a discussion of spatial and temporal coherence.) The latter property is understandable from the fact that ASE is basically amplified "noise." The bandwidth of ASE is typically a few times smaller than the gain linewidth $\Delta \nu$.

12.14 ULTRASHORT LIGHT PULSES

With mode-locked lasers it is possible to produce ultrashort, extremely intense pulses of radiation. Mode-locked lasers using saturable absorbers are used to produce, rather routinely, picosecond pulses with peak powers in some cases exceeding 10¹¹ W (100 GW). There are techniques for producing even shorter light pulses.

There are many scientific and technological applications of these ultrashort light

pulses. For instance, they can be used to study extremely fast photoprocesses in molecules and semiconductors. Especially promising applications may be possible in biological systems, where it has already been determined that certain fundamental chemical reactions occur on picosecond time scales. Intense laser pulses have also been of interest in connection with laser isotope separation and controlled thermonuclear fusion, and it seems safe to say that many new applications will be developed in the future. Not surprisingly, therefore, an entire field of research has grown up around the generation of ultrashort light pulses. Although it is well beyond our scope in this book to discuss in detail these developments, we will mention briefly some techniques in use.

One of these is the *colliding-pulse laser*. This is a mode-locked, three-mirror ring laser with two counter-circulating pulse trains (Figure 12.17). Pulses in each direction pass through a very thin (about 10 μ m) jet of a saturable absorbing dye. The absorption coefficient of the absorber is smallest when the intensity is largest. Therefore the cavity loss is least when the counter-circulating pulses collide and overlap within the thin dye jet. The thinness of the absorber forces the pulses to overlap within a very short distance and thus over a very short time interval ($\tau \sim 10 \ \mu\text{m/c} \sim 3 \times 10^{-14} \, \text{sec}$).

Another technique involves *chirping*, by which an ultrashort pulse from a laser can be further compressed. A *chirped* pulse is one in which the carrier frequency ω has a small time dependence. In particular, it has a linear time dependence of the form $\omega = \omega_0 + \beta t$. A pulse can be deliberately chirped by passing it through a medium with a nonlinear refractive index, i.e., a medium in which the refractive index depends upon the electric field (Chapter 17). The chirping results in a spectral broadening of the pulse, i.e., it extends the range of frequency components contained in the pulse. A chirped pulse can be compressed by passing it through a dispersive (i.e., frequency-dependent) *delay line*. If the higher-frequency components of the pulse travel more slowly than the lower-frequency components, the delay line is designed to make them catch up with the lower frequencies on the leading temporal edge of the pulse. By broadening the spectral width of the pulse by chirping, therefore, it is possible to narrow it in time.

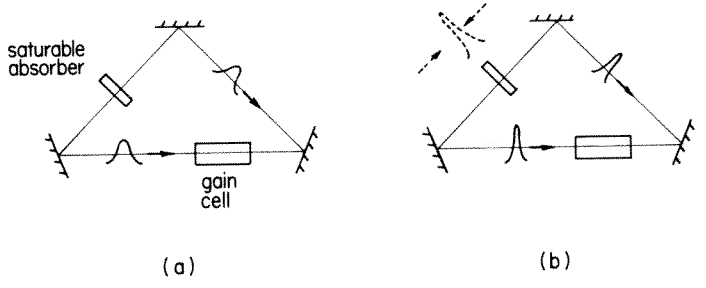


Figure 12.17 (a) A colliding-pulse ring laser with countercirculating pulses. (b) The lowest-loss condition is for the colliding pulses to synchronize and overlap inside the thin saturable absorber.

Optical pulses shorter than 10 fs (1 femtosecond = 10^{-15} sec) have been achieved by compressing in this way ultrashort pulses from a colliding-pulse dye laser.

APPENDIX 12.A RUNGE-KUTTA FORTRAN AND BASIC PROGRAMS

The Runge-Kutta algorithm is an easily implemented and frequently used method for the numerical integration of ordinary differential equations. For the first-order differential equation

$$\frac{dy}{dx} = F(x, y) \tag{12.A.1}$$

the fourth-order Runge-Kutta algorithm for y(x + h) is

$$y(x + h) = y(x) + \frac{1}{6}(k_1 + 2k_2 + 2k_3 + k_4)$$
 (12.A.2)

where

$$k_{1} = hF(x, y)$$

$$k_{2} = hF\left(x + \frac{h}{2}, y + \frac{k_{1}}{2}\right)$$

$$k_{3} = hF\left(x + \frac{h}{2}, y + \frac{k_{2}}{2}\right)$$

$$k_{4} = hF(x + h, y + k_{3})$$
(12.A.3)

The form of (12.A.2) and (12.A.3) is such as to duplicate the Taylor series for y(x + h) up to fourth order in the step size h. The method is easily extended to systems of equations, as in the example below.

The Runge-Kutta method is described in detail in many textbooks on mathematical methods and numerical analysis. For the reader's convenience we list here a FORTRAN program for the Runge-Kutta integration of the two coupled equations (12.4.4):

PROGRAM MAIN
DIMENSION Y(2), DY(2), W(2,5)
W IS A WORK ARRAY USED IN SUPPOSITION

C W IS A WORK ARRAY USED IN SUBROUTINE RUNG T=0,

Y(1) = 1.E - 3

Y(2) = 2.0

DT = .01

NSTEP = 1000

RETURN

END

```
DO 1 N = 1, NSTEP
    CALL RUNG(2,Y,DY,T,DT,W)
    CONTINUE
    PRINT 100,T,Y(1),Y(2)
100 FORMAT(3E16.7)
    STOP
     END
    SUBROUTINE DERIV (T,Y,DY)
    DIMENSION Y(2), DY(2)
    DY(1) = (Y(2) - 1.) * Y(1)
    DY(2) = -Y(1)*Y(2)
    RETURN
    END
    SUBROUTINE RUNG(N,Y,DY,T,DT,W)
    N IS THE NUMBER OF EQUATIONS
    DIMENSION Y(N), DY(N), W(N.5)
    DO 10 J = 1.N
10 W(J,1) = Y(J)
    CALL DERIV(T,Y,DY)
    DO 20 J = 1, N
   W(J,2) = DY(J)*DT
    Z=T+.5*DT
    DO 40 I = 2.3
    DO 30 J = 1, N
    Y(J) = W(J,1) + W(J,I)/2.
    CALL DERIV(Z,Y,DY)
    DO 40 J = 1.N
   W(J,I+1) = DY(J)*DT
    Z = T + DT
    DO 50 J = 1.N
   Y(J) = W(J,1) + W(J,4)
    CALL DERIV(Z,Y,DY)
    DO 60 J = 1.N
    W(J,5) = DY(J)*DT
    DO 70 J = 1.N
    Y(J) = W(J,1) + (W(J,2) + 2.*(W(J,3) + W(J,4)) + W(J,5))/6.
    T = T + DT
```

The dependent variables are stored in the array Y. In this case [Eqs. (12.4.4)] Y(1) = x and Y(2) = y. T is the independent variable (τ) , and the step size DT [denoted by h in (12.A.3)] is taken to be 0.01. In general DT should be taken small enough to give an accurate solution of the equations, but not so small that the program is unnecessarily time-consuming. The accuracy of the solution can always be checked by halving the step size and noting whether there is a significant change in the computed solution.

NSTEP is the number of integration steps. Each call to RUNG moves time

forward by DT. In the way our program is set up, therefore, the final values of Y after the last call to RUNG are $Y(1) = x(t_{max})$ and $Y(2) = y(t_{max})$, where $t_{max} = NSTEP*DT$. In general the intermediate values of Y can be stored in arrays for plotting purposes.

Subroutine DERIV simply defines the derivatives. In our example DY(1) = $dx/d\tau$ and DY(2) = $dy/d\tau$. Subroutine RUNG does a fourth-order Runge-Kutta integration, using the derivatives defined in DERIV. N is the number of (first-order) simultaneous differential equations to be solved; in our example N = 2. W is a work array that must be dimensioned N by 5. Only the MAIN and DERIV routines in our example depend on the specific problem, the RUNG subroutine being a "canned" routine, usable as it stands in every problem.

It may be worth noting that RUNG can also be used to solve higher-order differential equations of mixed order. For example, to solve the system

$$\frac{d^2x}{dt^2} + x = 0 x(0) = \left(\frac{dx}{dt}\right)_{t=0} = 1 (12.A.4)$$

using RUNG, we let Y(1) = x, Y(2) = dx/dt. Then (12.A.4) is equivalent to the two first-order equations

$$DY(1) = Y(2), DY(2) = -Y(1)$$
 (12.A.5)

with initial values Y(1) = Y(2) = 1.

RUNG can be used as it stands to solve complex as well as real systems of equations. One simply writes the equations of DERIV in complex form and declares the appropriate variables COMPLEX.

It is easy to convert the FORTRAN program above to a BASIC program. We list below a BASIC program suitable for use on many personal computers. The program is set up specifically to solve an autonomous set of equations of the type shown in Eqs. (12.4.4), where the right sides do not depend explicitly on the independent variable, but it can easily be modified to solve nonautonomous systems.

```
10
        DIM Y(2), DY(2), W(2,5)
20
        T=0
30
        N=2
40
        REM N IS THE NUMBER OF EQUATIONS
50
        Y(1) = .001
60
       Y(2) = 2
70
       DT = .01
80
       NSTEP = 1000
90
       FOR K=1 TO NSTEP
100
       GOSUB 1000
110
       NEXT K
120
       PRINT T, Y(1), Y(2)
500
       REM DERIV
510
       DY(1) = (Y(2)-1)*Y(1)
```

- 520 DY(2) = -Y(1)*Y(2)
- 530 RETURN
- 1000 REM INTEG
- 1010 FOR J=1 TO N
- 1020 W(J,1) = Y(J)
- 1030 NEXT J
- 1040 GOSUB 500
- 1050 FOR J=1 TO N
- 1060 W(J,2) = DT*DY(J)
- 1070 NEXT J
- 1080 FOR I=2 TO 3
- 1090 FOR J=1 TO N
- 1100 Y(J) = W(J,1) + W(J,I)/2
- 1110 NEXT J
- 1120 GOSUB 500
- 1130 FOR J=1 TO N
- 1140 W(J,I+1) = DT*DY(J)
- 1150 NEXT J
- 1160 NEXT I
- 1170 FOR J=1 TO N
- 1180 Y(J) = W(J,1) + W(J,4)
- 1190 NEXT J
- 1200 GOSUB 500
- 1210 FOR J=1 TO N
- 1220 W(J,5) = DT*DY(J)
- 1230 NEXT J
- 1240 FOR J=1 TO N
- 1250 Y(J) = W(J,1) + (W(J,2) + 2*(W(J,3) + W(J,4)) + W(J,5))/6
- 1260 NEXT J
- T = T + DT
- 1280 RETURN

APPENDIX 12.B DIFFRACTION OF LIGHT BY SOUND

The diffraction of light by sound waves can be understood by analogy with the diffraction of X-rays by crystals. The atoms of a crystal are spaced in a regular pattern, and consequently they scatter radiation cooperatively, with well-defined phase relations between the fields scattered by different atoms. This results in scattering only in certain well-defined directions, and the process is usually called "diffraction" instead of "scattering." Figure 12.18 shows a wave incident upon a stack of crystal planes separated by a distance d. The allowed diffraction angles are determined by the condition of constructive interference of the fields "reflected" from different planes. As shown in the figure, these diffraction angles satisfy the Bragg diffraction formula

$$2d \sin \theta = m\lambda, \quad m = 1, 2, 3, \dots$$
 (12.B.1)

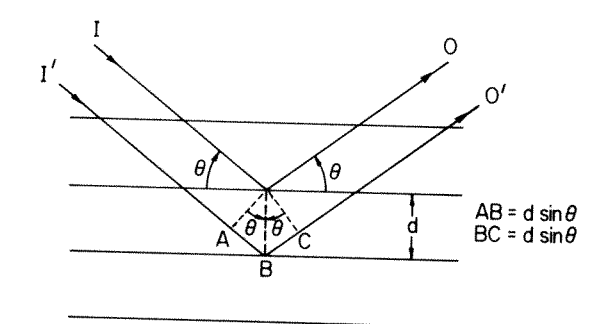


Figure 12.18 Diffraction of a plane wave by a stack of crystal planes. Constructive interference of the two rays IO and I'O' occurs when their path difference AB + BC is equal to an integral multiple m of the wavelength λ . This gives the Bragg diffraction formula $2d \sin \theta = m\lambda$ for the allowed diffraction angles θ . A more complete analysis shows that these angles give the *only* directions in which scattering occurs.

where λ is the wavelength of radiation and d is the separation distance between adjacent crystal planes.

• Since d is on the order of 1 Å in actual crystals, only wavelengths in the X-ray region can satisfy (12.B.1) and the requirement $|\sin\theta| \le 1$. The measurement of X-ray diffraction angles thus provides information about crystal structure. Indeed the use of crystals as "diffraction gratings" for X-rays has been one of the most important techniques of modern science for probing the structure of matter. This technique was originally suggested by Max von Laue. The idea arose in connection with the question of whether X-rays were particles or waves. L. Brillouin predicted the diffraction of radiation by sound waves in 1922, and it was first observed ten years later by P. W. Debye and F.W. Sears. •

The refractive-index variation associated with a sound wave of wavelength λ_s has a spatial dependence of the form

$$\Delta n(x) = a \sin k_s x \tag{12.B.2}$$

where $k_s = 2\pi/\lambda_s$ and a depends on material constants of the medium and the intensity of the sound wave. Equation (12.B.2) arises from the fact that a sound wave is basically a wave of density variation. Figure 12.19 shows an intuitive way of understanding the diffraction of light by a sound wave. We regard the planes of constant x where (12.B.2) is a maximum as "crystal" planes which, because of their regular spacing λ_s , will diffract light only in certain well-defined directions. Indeed it turns out that the diffraction angles are given by the Bragg formula (12.B.1) with $d = \lambda_s$ and m = 1:

$$2\lambda_s \sin \theta = \lambda/n \tag{12.B.3}$$

We have included the effect of the refractive index n of the medium.

The important difference between (12.B.1) and (12.B.3) is that there are no higher-order diffraction angles corresponding to m > 1 in (12.B.3). This differ-

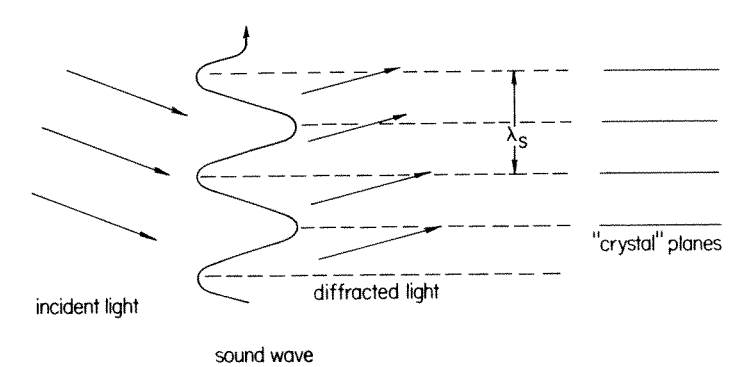


Figure 12.19 Intuitive picture of diffraction of light by sound as diffraction from a fictitious set of "crystals" planes defined by the intensity maxima of the sound.

ence arises from the fact that the "diffraction grating" associated with the sound wave indicated in Figure 12.19 is really a spatially continuous one, not a discrete set of crystal planes with nothing in between.

Equation (12.B.3) gives only the diffraction angle. It does not tell us the strength with which the sound wave diffracts light, i.e., the fraction of light intensity diffracted after a given distance of propagation. This is determined by a and the wavelength of the light.⁴

PROBLEMS

- 12.1 (a) Write the steady-state solutions of equations (12.2.5) in such a way as to show the saturation of \overline{N}_2 with increasing \overline{I}_{ν} .
 - **(b)** Verify the equations (12.3.16) and (12.3.17) for the period and lifetime of relaxation oscillations.
- **12.2** (a) Show that the quantity x defined in Eq. (12.4.1) is the cavity photon number density divided by the threshold population inversion density.
 - **(b)** Show that Eqs. (12.2.5) may be written as (12.4.4) when the change of variables (12.4.1)–(12.4.3) is made.
- **12.3** (a) Why is it that so much more power can be obtained from a *Q*-switched laser than in ordinary continuous-wave operation?
 - **(b)** Suppose a *Q*-switched laser using a rotating mirror or a saturable absorber is pumped continuously. How do you expect the laser to behave?
- 12.4 Set up the equations for x and y [Eqs. (12.4.1) and (12.4.2)] in the case
- 4. See, for example, R. Adler, "The Interaction between Light and Sound," *IEEE Spectrum*, May 1967, p. 42.

where Q switching is done with a saturable absorber with absorption coefficient $a=a_0 \ (1+I/I^{\rm sat})^{-1}$. If you have access to a computer, solve these equations numerically using, for example, the Runge-Kutta algorithm of Appendix 12.A. You will have to assume values of the small-signal absorption coefficient a_0 and the saturation intensity $I^{\rm sat}$ of the absorber. Determine how x and y depend on the choice of a_0 and $I^{\rm sat}$.

- 12.5 (a) Suppose we have N oscillators whose frequencies are given by (12.7.2) and whose phases ϕ_m are fixed but not "locked" according to (12.7.10). Discuss the properties of the sum X(t) of the oscillator displacements in this case. Can the maximum value of X(t) be as large as in the phase-locked case?
 - (b)*Suppose that the phases ϕ_n are randomly chosen from an ensemble and are completely uncorrelated, so that $\langle e^{i(\phi_m \phi_n)} \rangle = \delta_{mn}$, where $\langle \cdot \cdot \cdot \rangle$ indicates an ensemble average. Then compute $\langle X(t) \rangle$ and $\langle X^2(t) \rangle$.
- **12.6 (a)** Show that each pulse of a mode-locked pulse train has an intensity *N* times larger than the sum of the intensities of the individual modes constituting it.
 - **(b)** Show that the average intensity of a mode-locked pulse train is equal to the sum of the intensities of the individual modes constituting it.
- Make a plot of the time-dependent factor in the brackets in Eq. (12.9.5), choosing $\phi_m = 0$, $\Omega = \omega_m/10$, and (a) $\epsilon = \frac{1}{2}$, (b) $\epsilon = 1$, (c) $\epsilon = 5$.
- 12.8 Consider the 6328-Å He-Ne laser.
 - (a) Estimate the shortest pulse that can be obtained by mode-locking such a laser.
 - **(b)** What is the duration of each pulse of the mode-locked train if the gain tube has length l = 10 cm and the mirror separation L = 40 cm?
 - (c) What is the separation between the mode-locked pulses in part (b)?
 - (d) Why do liquid dye and solid-state lasers produce much shorter mode-locked pulses than typical gas lasers?
- 12.9 (a) Estimate the average power, in watts, expended by a normal human adult. Assume that a "normal human adult" consumes 2500 dietitian's calories $(2500 \times 4185 \text{ J})$ per day, and that his output energy just balances his input energy.
 - (b) Estimate the intensity at a distance of 1 m from a 60-W light bulb.
 - (c) Estimate the average electrical power used to operate a typical house in your area.
- 12.10 It is possible to "dump" the cavity of a pulsed laser by making the reflectivity of the output mirror effectively zero at the moment of peak intensity. What is the advantage of "cavity dumping" in this way?